Measurements of ^{239}Pu and ^{235}U Fission Product Decay Power From 1 to 10^5 Seconds

EPRI

EPRI NP-998
Project 766-1
Final Report
September 1979

Keywords:
^{239}Pu Decay Power
^{235}U Decay Power
Fission Product Decay Power
Gamma and Beta Decay Power

Prepared by
IRT Corporation
San Diego, California

Measurements of ^{239}Pu and ^{235}U Fission Product Decay Power From 1 to 10^5 Seconds

NP-998
Research Project 766-1

Final Report, September 1979

Prepared by

IRT CORPORATION
7650 Convoy Court
San Diego, California 92111

Principal Investigators
S. J. Friesenhahn
N. A. Lurie

Prepared for

Electric Power Research Institute
3412 Hillview Avenue
Palo Alto, California 94304

EPRI Project Managers
F. J. Rahn
W. Eich
Nuclear Power Division

EPRI PERSPECTIVE

In 1971, the American Nuclear Society Standards Subcommittee 5 (ANS-5) proposed the adoption of a standard entitled "Decay Energy Release Rates Following Shutdown for Uranium-Fueled Thermal Reactors." This proposed standard has subsequently been referenced in Appendix K of 10CFR50. By virtue of Nuclear Regulatory Commission (NRC) requirements, it is now specified as part of the emergency core cooling system (ECCS) evaluation models, with the heat generation rate from the radioactive decay of fission isotopes assumed to be equal to 1.2 times the values appearing in the standard. The factor 1.2 appears to be based on the uncertainty quoted in the standard for short cooling times. Subsequent experimental and computational work has somewhat lowered the magnitude of the decay heat values at short times after reactor shutdown and has significantly reduced its uncertainty. As a result, another decay heat standard has been developed and approved by ANS-5 and is in the process of being issued. Presumably, this new standard will be incorporated by the NRC into its regulations.

This project is one of several EPRI projects (see also EPRI reports NP-180, NP-161, and NP-997) that provided supporting experimental work for use in the development of the new ANS-5 Standard. The report presents total decay heat data for various length irradiations of ^{239}Pu and ^{235}U. Particular emphasis was given to the ^{239}Pu results because a large fraction of the fissions in high exposure fuel is due to ^{239}Pu. In order to remove some remaining experimental discrepancies and to provide data for checking the so-called "summation" calculations used to predict decay power under specific reactor operating conditions, spectral (i.e., energy) measurements were also obtained. These results will be reported in EPRI report NP-999.

This report should be of interest to individuals in utilities concerned with the licensing of nuclear units. It is also of interest to utility personnel evaluating LOCA-type accident scenarios and to researchers investigating decay heat in nuclear reactors.

Walter Eich, Project Manager
Safety and Analysis Department
Nuclear Power Division

ABSTRACT

The absorbable components of the fission product decay power from thermal neutron fission of ^{239}Pu and ^{235}U have been measured in the 1 to 10^5 second cooling time interval. Irradiation times for ^{239}Pu were 1000 seconds and 24 hours; for ^{235}U they were 1000 seconds, 20,000 seconds, 24 hours and 35 days. The measurements were made using a "nuclear calorimeter" which is based on a large (4000 ℓ) liquid scintillation detector capable of detecting a large fraction of the fission product decay energy. Separate beta and gamma-ray contributions to the total decay power were determined.

ACKNOWLEDGMENTS

The authors would like to acknowledge the advice and consultation of Dr. Charles Preskitt and the assistance of Mr. William Gober in mechanical apparatus fabrication. We would also like to thank J. K. Dickens and J. W. McConnell of ORNL for assistance in the ^{239}Pu normalization, and T. England of LASL, B. Spinrad of OSU, and R. Schenter and F. Schmittroth of HEDL for providing the results of their calculations.

CONTENTS

ILLUSTRATIONS

TABLES

SUMMARY

The operation of a power reactor causes the formation of a large variety of radioactive nuclei in the core as the result of the nuclear fission process. These fission products accumulate to the point where several percent of the reactor heat generation results from the decay of these products. When the reactor is shut down for any reason, this heat must be removed in order to prevent damage to the core.

In the event of a primary cooling system failure, the capabilities required of the backup cooling systems, as well as the analysis of the events following a subsequent backup cooling system failure, depend upon an accurate knowledge of this heat source. Before the start of the present set of measurements the uncertainty in the decay heat for design purposes was as large as 40 percent.

The present measurements are designed to provide test cases for calculations of decay heat by computer codes. These codes can then be used to calculate the decay heat for any given reactor operating history.

The initial fuel loading of a reactor usually contains the fissionable isotope ^{235}U along with the more abundant ^{238}U. As the reactor is operated a significant quantity of the fissionable isotope ^{239}Pu is formed by neutron absorption in ^{238}U. For this reason the present work comprises measurements of the decay heat released by ^{235}U and by ^{239}Pu. The measurements involve the irradiation of a sample in a constant neutron flux for time periods varying from 1000 seconds to 35 days. At the end of irradiation the sample is transferred to a very large scintillator in less than one second. The scintillator detects the beta and gamma radiation which constitutes virtually all of the decay heat from the fission products in the sample. The scintillator output is recorded by a computer over a period of one day.

The scintillator is calibrated with a radioactive source of known strength, and the fission rate that existed in the sample is determined by an auxiliary experiment. This allows the scintillator output to be converted to energy emission rate per fission per second.

The techniques used in these measurements are unique in decay heat measurements. The time span of the measurements, the variety of irradiation times and the accuracy achieved exceed that previously reported in any previous measurements. The results reported here will allow a significant reduction in decay heat uncertainty and hence result in significant savings in future plant construction costs.

Section 1

INTRODUCTION

The past several years have seen a highly concentrated effort focused on the improvement of our knowledge and understanding of fission product decay power. This effort has included both analytical work to improve the data base and to pinpoint the sources of uncertainty in the calculations of decay power, and new measurements to serve as benchmarks for verifying the calculations. The motivation for all of this was the recognition that the very significant uncertainties that existed prior to the present generation of measurements and analyses imposed an economic penalty on nuclear power plant design, requiring very conservative allowances for decay power load. This was particularly true in the short cooling region (<1000 seconds).

Historically, the importance of knowing the power produced by the decay of radioactive materials in the reactor was recognized early, and many schemes have been used for estimating this quantity. In addition to fission product decay power, there is also decay heat produced by the transuranics and activation products in the reactor. The fission products, however, constitute the major contribution to the decay power.

The concentrations of fission products and thus their energy release rates are dependent upon the fuel composition, neutron spectrum and irradiation history of the fuel. For this reason we depend on analytical methods for determination of decay power in specific safety analyses or other applications. Over the years good computational tools have been developed for generating energy release rates or decay power information. Recent reviews of the historical development are given by Bjerke et al. (1) and Schrock (2).

The principal computational method in use today is the summation method. As the name implies, contributions to the energy release rate from the individual fission products as a function of irradiation conditions and time are summed. This method requires an extensive library of nuclear data for the fission products, and the

data library constitutes the primary limitation of the accuracy of the summation method. Considerable effort has been devoted to quantifying the uncertainties in the summation calculations (1, 3-6).

Traditionally, there have been two basic measurement techniques for determination of decay heat. One is a radiometric method in which the beta and gamma radiations are detected directly in a low geometry experiment. The other method is calorimetric measurement of heat produced by the absorption of the radiation in a massive absorber. A determination of the number of fissions in the sample must be made in either case.

A unique method of measuring the decay power was developed by the present authors that utilizes the advantages of both the radiometric and calorimetric techniques (7). The fissile materials are irradiated in a neutron flux produced by a water moderated ^{252}Cf source. The fission product decay radiation is detected in a large liquid/plastic scintillation detector that absorbs nearly all the beta and gamma radiations and produces a light signal proportional to the energy absorbed. The fission rate is measured in a specially designed ion chamber. The fast response of this method allows accurate tracking of the rapid decay at early cooling times (as early as 1 second after irradiation), and the large detector size minimizes the reliance upon calculated corrections for undetected energy. Thus, the system behaves as the nuclear analog of the thermal calorimeter.

The output of the "nuclear calorimeter" is calibrated in terms of energy emission rate using a ^{60}Co source whose calibration is traceable to the National Bureau of Standards. The measured cooling time dependence of the fission product energy release is divided by the fission rate in the sample during irradiation to produce an energy release per fission versus cooling time.

The present work is a continuation and extension of the work previously reported on ^{235}U (7). New measurements of the ^{239}Pu decay power have been completed; the ^{235}U results have been improved and extended to longer and shorter irradiation times. The plutonium decay power is of interest not only for possible future use in mixed oxide fuel cycles, but also because it contributes a significant fraction of the decay power in present fuel cycles at high burnup.

In an attempt to provide a wide range of experimental data with which to test the calculations, data were taken for four different irradiation times (1000 seconds,

20,000 seconds, 24 hours and 35 days) for ^{235}U, and two irradiation times (1000 seconds and 24 hours) for ^{239}Pu. These different irradiation times place emphasis on different fission product nuclides.

In the following sections the experimental methods and apparatus are more fully described. The primary method used for measurement of the fission rate, as described in Section 3, was independently verified for a ^{239}Pu sample at another laboratory using a different technique. The results are in excellent agreement. The data analysis procedures, including corrections to the data and an assessment of the uncertainties in the experiment are given in Section 4. Finally, the results are presented and discussed and compared to other measurements and calculations.

Section 2

EXPERIMENTAL APPARATUS AND PROCEDURES

2.1 SAMPLES

The fissile materials used in the decay heat measurements were purchased from Oak Ridge National Laboratory. Both the uranium and plutonium were alloyed with aluminum. The uranium sample composition is 22.8 weight percent uranium and the balance aluminum, rolled to a thickness of approximately 10 mg/cm^2. The plutonium sample is composed of 98 weight percent plutonium and the balance aluminum with a thickness of 14 mg/cm^2. The isotopic compositions of the fissile elements as measured by the supplier are given in Table 2-1.

Table 2-1

ISOTOPIC ANALYSIS OF FISSILE MATERIALS

Uranium		Plutonium	
Isotope	Atomic Percent	Isotope	Atomic Percent
234	1.113	239	98.76
235	93.26	240	1.2
236	0.259	241	0.04*
238	5.37		

*Analysis by gamma-ray spectrometry yielded 0.024% (8)

2.2 SAMPLE ENCAPSULATION

The requirements for sample encapsulation for this experiment are quite severe. The fissionable material must be contained in an enclosure that satisfies the following requirements:

1. All fission products must be retained in the sample, including the gaseous isotopes.

2. The encapsulation must be thin enough to allow the majority of the beta and gamma energy to escape with minimum perturbation.

3. The neutron activation of the encapsulation must be minimal.

4. The encapsulation must allow the sample to be presented to the scintillator with a large solid angle to minimize positioning errors.

5. The encapsulation must be mechanically sturdy enough to withstand the shock of being transported by a high speed pneumatic transfer system.

These requirements were satisfied with the encapsulation illustrated in Figure 2-1. The fissionable material in the form of a thin metallic foil was laminated between two sheets of 0.0051-cm thick Mylar which had been roughened by sanding and coated with Pliobond contact cement. The bonding was completed by hot pressing at 100°C for 30 minutes. This laminate was stiffened by adding formed strips of 0.0178 cm Mylar at the edges. This assembly was in turn cemented in the tapered end of a high density polyethylene rabbit. The cementing was accomplished by drilling holes in the Mylar block and the end of the rabbit which allowed good mechanical coupling of these two parts by Shell 820 epoxy cement without reliance on surface adhesion.

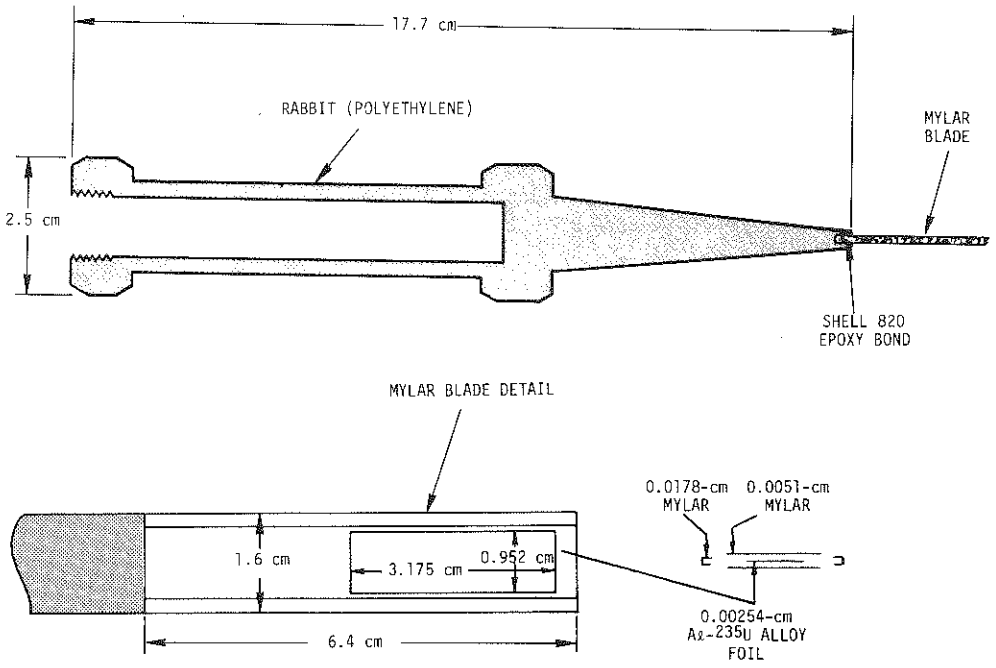

Figure 2-1. Polyethylene rabbit and fissile sample

The shoulders on the rabbit provide indexing guides through the pneumatic transfer tube, and the elongated neck allows the sample to be projected deeply into the reentrant hole in the scintillator, which provides a large solid angle. The cover material is thin enough to provide good beta energy transmission above 100 keV beta energy, and yet is thick enough to retain all fission products.

The impervious nature of this encapsulation was confirmed in four independent ways:

1. A bare ^{235}U foil was irradiated at the end of an evacuated tube. Evacuation was via a liquid nitrogen cooled copper chamber, adjacent to which was located a Ge(Li) gamma spectrometer. Several prominant lines from noble gas fission products were observed. The experiment was repeated with a foil encapsulated as above, and the peak areas were less than 10% of those measured with the bare foil. Some of these counts may have been due to residual contamination from the bare foil run.

2. A decay heat measurement was performed with the usual encapsulation and an iron liner inside the scintillator to cause only the gamma-ray component to be recorded, which, of course, is insensitive to cover thickness. This same foil was allowed to cool several days and the thickness of the mylar cover increased by the addition of a 0.0178 cm cover on both sides. The decay heat measurement was repeated with identical results.

3. An encapsulated foil was irradiated and the decay of the 250 keV ^{135}Xe line was measured over a period of 100 hours. The experiment was repeated with a foil which was cast at the center of a block of epoxy resin. The minimum leakage path for this "leak proof" sample was 0.4 cm. The time history of the ^{135}Xe line was observed to exhibit the same time behavior as the previous foil.

4. In order to check for possible leakage due to the mechanical shock of the rabbit system operation, a decay heat measurement cycle was interrupted periodically and the 250 keV ^{135}Xe line area measured. The area followed the expected decay curve with a precision of ±20%. The uncertainty was due largely to interfering fission product lines.

The activation of the Mylar blade assembly and polyethylene rabbit is negligible in all cases with the exception of the ion chamber normalization measurement to be discussed later in which very small quantities of material are used.

2.3 IRRADIATOR

The neutron source for these measurements was a 10-mg ^{252}Cf located in a lead block $\approx$2 cm thick to reduce the gamma flux. This lead block is located near the bottom of a 2-meter deep water-filled well. The water in the irradiation well is continuously purified through a pump and filter. The source is immediately adjacent

to a 10-cm diameter dry tube positioned at the vertical axis of the well. This dry tube accommodates a 2.8-cm diameter aluminum tube which is one end of a pneumatic transfer system. This small tube is surrounded by polyethylene rings which position it at the center of the dry tube and provide additional neutron moderation. The neutron flux at the sample position is approximately 10^8 n/cm^2/sec.

The rabbit is irradiated with the sample-containing blade upward and with the neutron source at the same elevation as the sample. At the conclusion of the irradiation the computer controlling the experiment applies air pressure to blow the sample toward the scintillator. The computer starts the cooling time calculation from the instant the rabbit sense switch located in the irradiator indicates that the rabbit is gone.

2.4 PNEUMATIC TRANSFER SYSTEM

The pneumatic transfer system is activated by a fast-acting bidirectional solenoid valve that vents air from a storage tank into the system. The storage tank is maintained at 0.4 ± 0.07 kg/cm^2 by means of a specially constructed pressure switch and solenoid valve which admits air as required from a high pressure supply line. This pressure was chosen to cause the air valve on-time to comprise approximately half the total rabbit transfer time ($\approx$0.8 sec). This choice seems to provide the most reliable operation. The connection between the irradiator and scintillator is via 2.8-cm ID polyethylene tubing which is interrupted at its center by a receiver mechanism.

The receiver has a pass-through tube which allows direct transfers from irradiator to scintillator, and six storage tubes which are used to store rabbits coming from the scintillator during background and calibration phases of the measurement. The receiver also contains a special rabbit on which is mounted a standard ^{60}Co source. This source is used to calibrate the scintillator during the course of the measurements.

2.5 NUCLEAR CALORIMETER

The 4000 liter liquid scintillator used in the present measurements was originally constructed as a gamma-ray detector used in neutron capture cross section measurements (9). It is of modular design and consists of 44 thin walled plastic cylinders filled with a decahydronapthalene-based liquid scintillator. These cylinders (called logs) are 2 meters long and 23 cm in diameter with a 23-cm

nonscintillating region at each end. Each cylinder is wrapped with aluminum foil, and hence operates as an individual light pipe. It is viewed on each end by a 12-cm diameter photomultiplier tube.

A 61-cm diameter cylinder with a 15-cm diameter axial hole is located at the center of the log array. This "center section" is similar to the logs except that it is viewed by eight photomultipliers on each end. The liquid scintillator is illustrated in Figure 2-2.

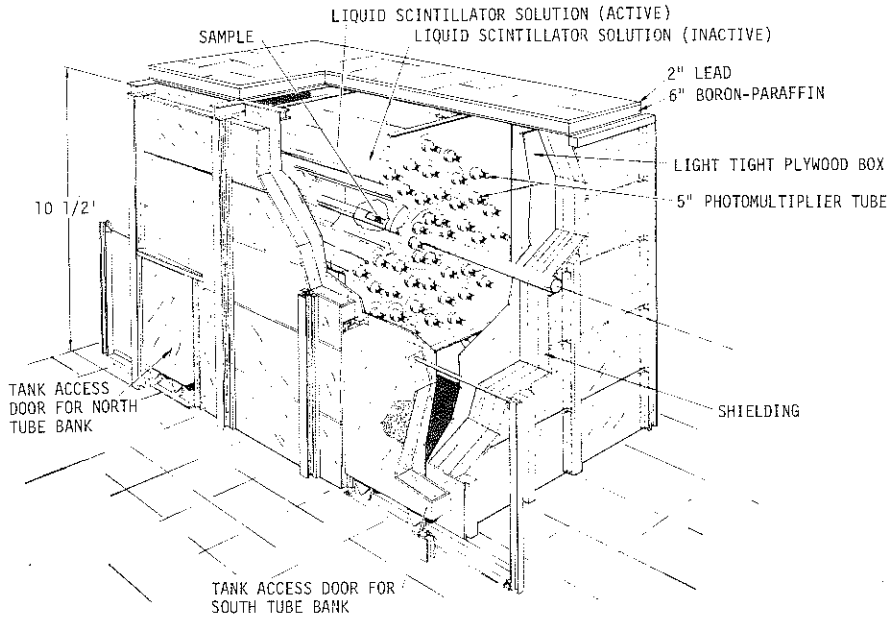

Figure 2-2. Illustration of scintillator construction

For the present work a 40-cm long, 15-cm diameter NE 110 plastic scintillator was located in this axial hole at the geometric center of the liquid scintillator. This plastic scintillator was constructed with a reentrant hole which forms the terminus of the rabbit system. The rabbit system is thus able to introduce the sample into the scintillator without any intervening material. The reentrant hole is polished, but is operated without any light reflector. Response function investigations indicated excellent agreement between the ^{137}Cs Compton edge from the 662 keV gamma ray versus the 630 keV internal conversion line. This tends to confirm the linear response of the system for energetic beta particles, but the

surface damage due to polishing can be expected to produce a slightly nonlinear response at lower energies, as evidenced in Figure 2-3.

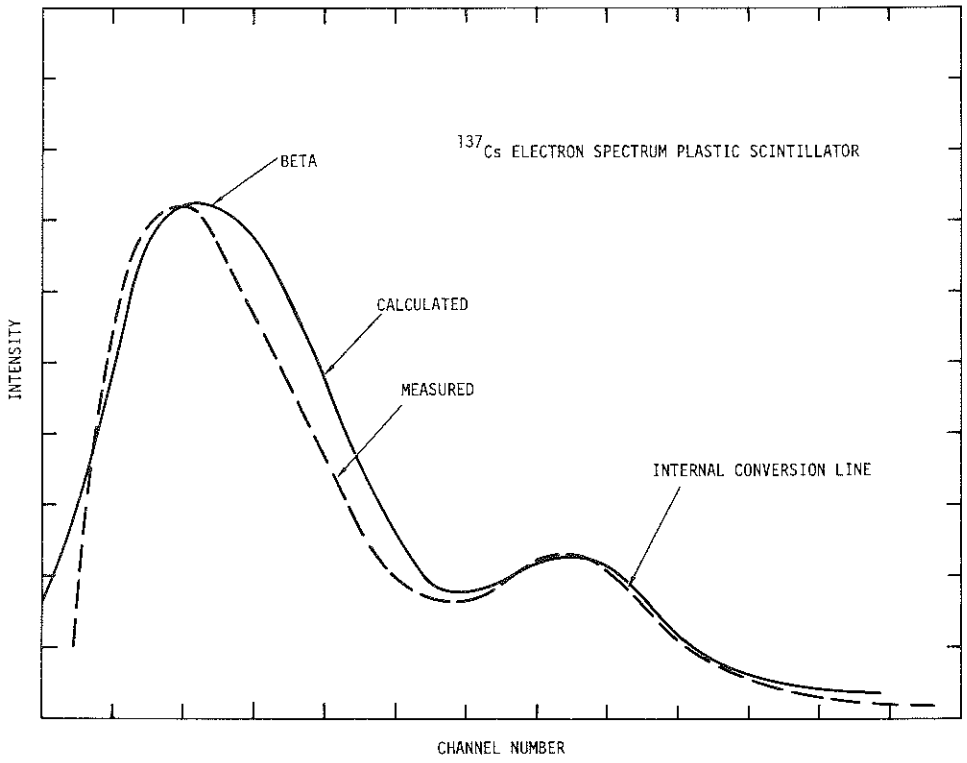

Figure 2-3. Calculated versus measured ^{137}Cs electron spectrum in plastic scintillator

The plastic scintillator is viewed by a 12-cm diameter photomultiplier on one end and four 5-cm diameter photomultiplier tubes surrounding the rabbit tube on the other end. These five photomultiplier tubes are connected in parallel and constitute the "plastic scintillator" signal. The 16 photomultipliers on the 61-cm diameter cylinder are summed to form the "center section" signal and the 88 photomultipliers on the 23-cm diameter scintillators are summed to form the "log" signals.

These three sum signals are routed via computer controlled relays to a common summing point at the input of a Keithly 410 electrometer. The computer is thus able to select individual regions of the scintillator in the course of the experiment. This feature allows the computer to adjust the net plastic scintillator

signal from the ^{60}Co standard source to a predetermined fraction of the signal from the center section. This adjustment is made periodically during the experiment with a precision of $\approx$2% to ensure a constant beta/gamma sensitivity of the system. The relative signal from the logs is reported to the operator, but the adjustment of this signal is manual.

The response from each of the 109 photomultipliers in the system is adjusted using the Compton edge from the 4.4 MeV gamma ray from a 1 Ci PuBe source located at the center of the scintillator. The 1.57 MeV ^{142}Pr line is used to adjust the overall response of the center section versus the logs. For a more detailed description of the scintillator see References 7, 9, and 10.

2.6 SIGNAL PROCESSING

The negative signals from the three regions of the scintillator are brought to a common summing point at the input to the electrometer along with a positive bucking current. This bucking current is adjusted via a computer-controlled power supply to cause the net current to fall at the lower end of the measurement range. This allows the high resolution measurement of small signals in the presence of large ambient signals.

The output from the electrometer is routed to a 10-millisecond RC integrating circuit and an operational amplifier which increases the 5 V electrometer output to 10 V. This amplified output is routed to an 8192 channel Hewlett-Packard 5416B analog-to-digital converter (ADC). The computer reads the output of the ADC in the sample mode. The results of 500 to 20,000 samples are averaged each time a command to read the scintillator signal is given.

A schematic of the signal processing is illustrated in Figure 2-4.

2.7 DATA ACQUISITION SYSTEM

All phases of data acquisition are under the control of a Hewlett-Packard 2116B computer system. The acquisition code logic diagram is illustrated in Figure 2-5. The data acquisition code reads the birth dates of the standard source and any decay heat samples which may already be in the system. It also reads the rabbit system operating parameters and a table of cooling times at which decay heat data points are to be taken. When the time for a data point arrives, the computer adjusts the bucking voltage and plastic scintillator gain using the ^{60}Co rabbit,

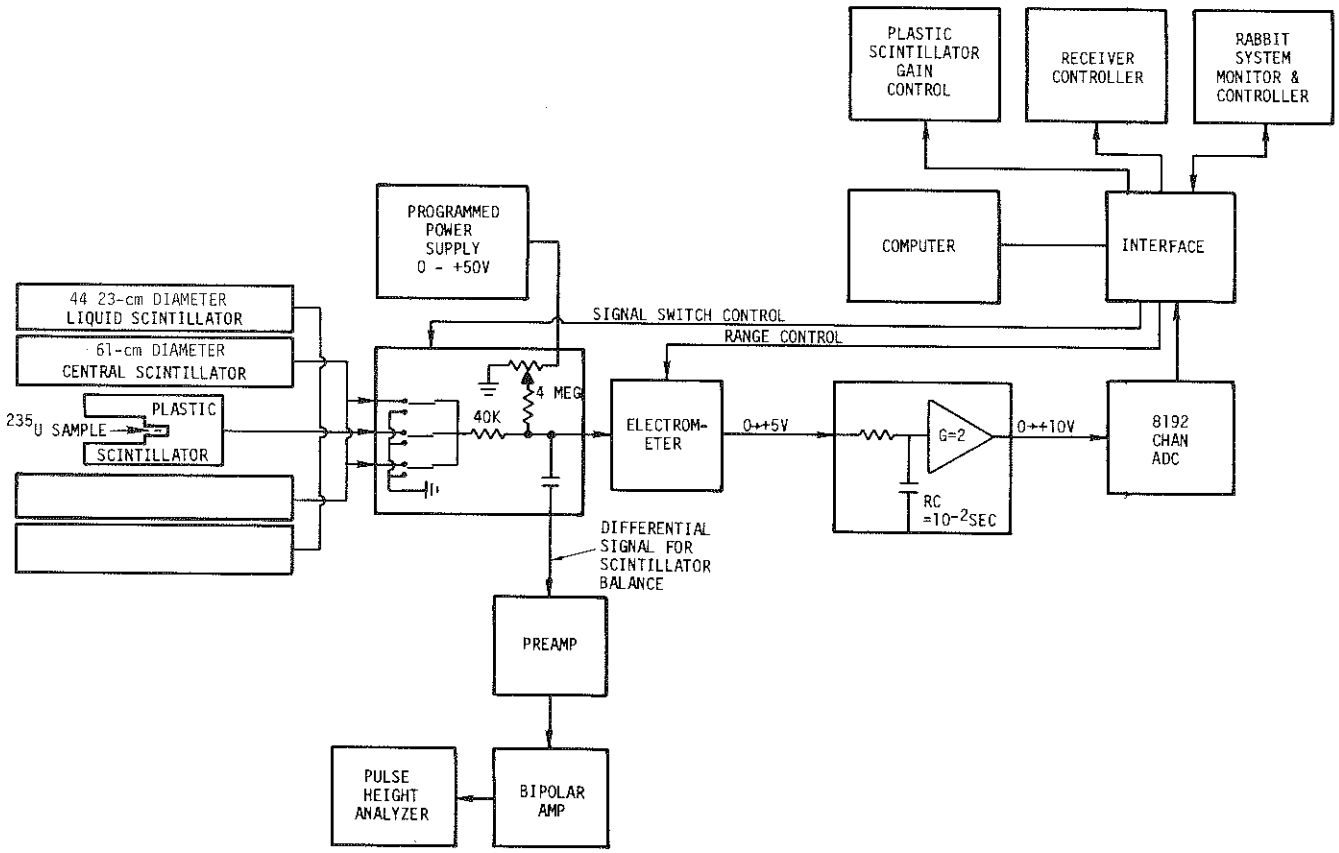

Figure 2-4. Signal processing diagram

and then measures the sample-out background. The ^{60}Co rabbit is then re-inserted into the scintillator and the net signal determined. The ^{60}Co rabbit is cycled 5 to 20 times, and the mean value and standard deviation estimates are computed. Any points greater than two standard deviations from the mean are rejected and the computations repeated.

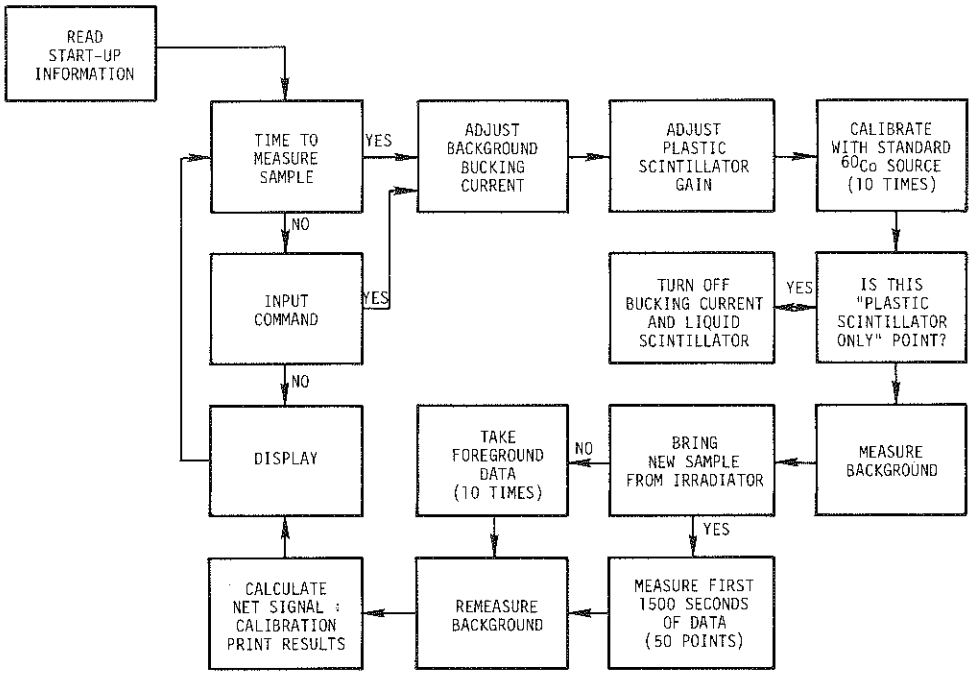

Figure 2-5. Logic diagram of data acquisition code

The net signal with its uncertainty is corrected for the 5.261-year ^{60}Co half life and is stored as the scintillator calibration signal. The cycling process is then repeated using the sample being measured. The ratio of the net sample signal to the calibration signal is taken to be proportional to the energy emission rate from the sample.

In order to obtain an accurate record of the rapid decay during the first 1500 seconds of decay, the cycling procedure is not used during this time period. The system is calibrated and the background measured before the sample is brought from the irradiator. The sample then remains in the scintillator as the computer

records the decay heat signal using a logarithmic time mesh. The standard deviation in this initial time period is estimated from the variance of the points, the variance in the calibration, and the change in the calibration over this time period.

Section 3

FISSION RATE DETERMINATION

In order to convert the sample energy release rate into decay heat it is necessary to determine the fission rate that existed in the samples. Since these fissions are not directly observable, an auxilliary experiment must be performed to measure the sample fission rate. Two independent methods have been used for the plutonium decay heat studies. The first is an ion chamber cross-calibration technique that was used in previous decay heat measurements on ^{235}U (7, 11); the other is a fission product gamma-ray counting method performed at Oak Ridge National Laboratory (8).

3.1 ION CHAMBER METHOD

This technique involves the irradiation of a very small quantity of the fissionable material in an ion chamber. The fissionable material is evaporated to a thickness of approximatley 100 micrograms/cm^2 on a very thin nickel substrate (500 micrograms/cm^2). The isotopic composition of the fissile material is given in Table 3-1. The deposit and substrate are mounted on a rabbit assembly as illustrated in Figure 3-1, and introduced into the ion chamber illustrated in the same figure. As an experimental convenience, the same neutron field is used to irradiate the ion chamber as that used to irradiate the larger foils. The thin substrate and the 4π geometry of the chamber allow the direct counting of the fission events with high counting efficiency.

The chamber is constructed almost exclusively of plexiglas to reduce electrical leakage problems encountered in high radiation fields. The foil-containing rabbit is lowered through a hole in the top of the chamber, and the foil allowed to contact a high negative voltage terminal mounted on the bottom of the chamber. A Frish grid operated at ground potential improves pulse height resolution. Field shaping electrodes not shown in Figure 3-1 are mounted parallel to the edges of the foil and are operated at an intermediate negative voltage to improve ion collection. The collector plates are connected in parallel to the input of the preamplifier and are operated at a positive potential.

Table 3-1.

ION CHAMBER FOIL ASSAY

^{235}U Foils		^{239}Pu Foils	
Isotope	Atomic Percent	Isotope	Atomic Percent
^{233}U	<0.0005	^{238}Pu	<2 ppm
^{234}U	0.034	^{239}Pu	99.107
^{235}U	99.89	^{240}Pu	0.877
^{236}U	0.025	^{241}Pu	0.011
^{238}U	0.052	^{242}Pu	0.005
		^{244}Pu	<0.0005

The neutron gradient in the chamber was measured by gold foil activation and found to be quite small; thus minor positioning errors have a negligible effect on the fission rate. The measured fission rate for a given foil has been observed to follow the ^{252}Cf decay to within 1% over a period of several months.

The signals from the chamber are amplified via a bipolar shaping amplifier with 0.25 μs time constant. The gain is adjusted so that the majority of the fission events produce 4x overload in the amplifier. This allows the low energy portion of the pulse height distribution to be examined in detail. An example of such a distribution is shown in Figure 3-2. The background illustrated in the figure was obtained by wrapping the chamber with 0.02 cm cadmium. The background at low pulse heights is dominated by alpha particles and recoil protons from fast neutrons. The background distribution contains some thermal neutron fission events but this has no effect on the shape of the net distribution. The chamber is always operated with an aluminum foil cover to exclude electrical noise.

The pulse height interval designated as "fit region" in the figure is fitted to a second order polynomial, and the area below the lowest reliable data point is calculated to obtain the best estimate of the bias efficiency. The bias efficiencies thus obtained vary from 95 to 97%. A linear fit typically agrees with the second order fit to within 0.5%.

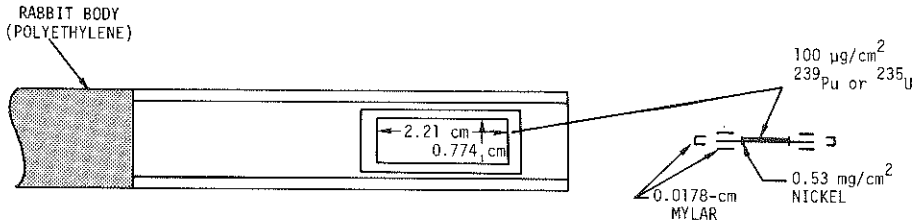

Figure 3-1(a). Detail of rabbit and sample assay.

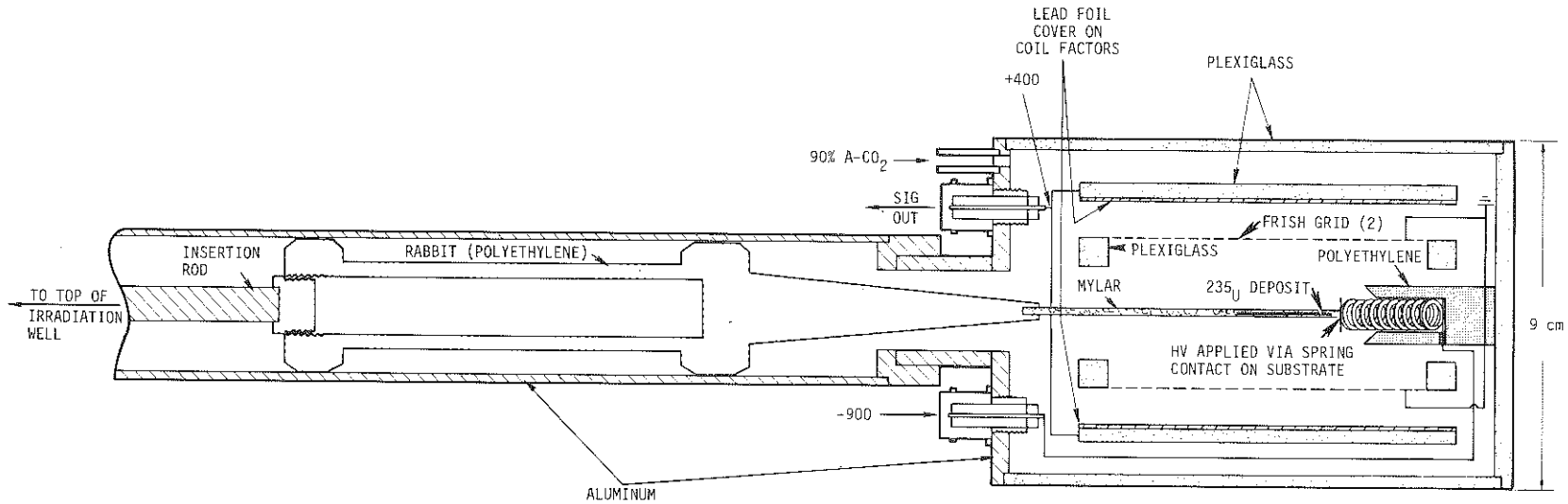

Figure 3-1(b). Ion chamber construction

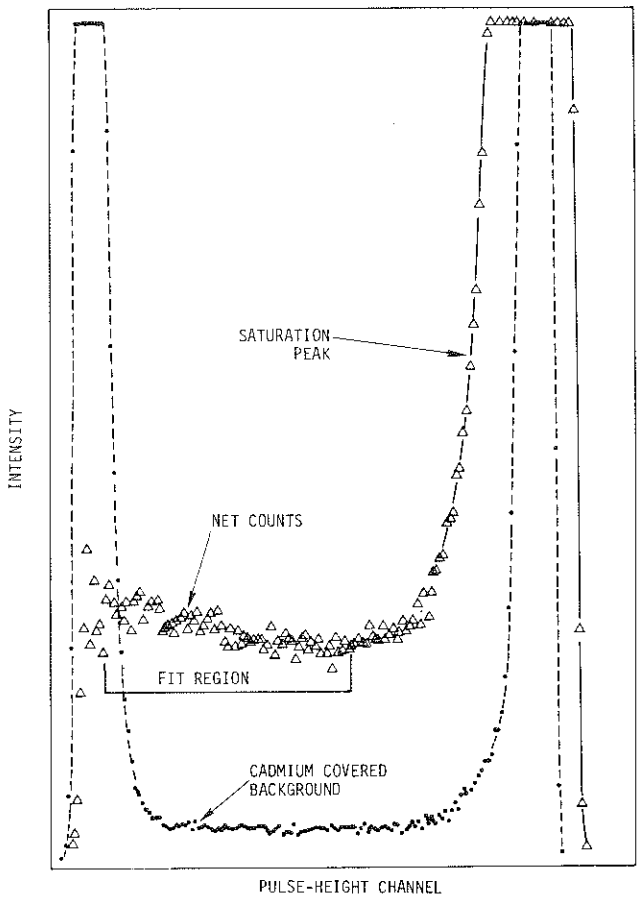

Figure 3-2. Ion chamber pulse height distribution for ^{239}Pu

Once the efficiency has been determined, the electronic bias is raised to the midpoint of the distribution to exclude the majority of the background, and the bias efficiency change at this higher bias is calculated from the measured distribution. The fission rate is then measured and corrected for dead time using the superimposed test pulse technique. A small background as measured with a blank rabbit is subtracted to obtain the net fission rate.

We now enter a second phase of the measurement in which the scintillator response to the fission products from this fission rate is measured. In order to do this we confine the fission products in the foil by applying two layers of 7 mg/cm^2 polyester tape to each side. After waiting for any residual fission product activity to decay, the background from the foil is measured in the scintillator in a manner identical to that used for the large fission heat samples. The foil is

then returned to the chamber and irradiated for a time identical to that used for the large foil irradiations.

This irradiated ion chamber foil is introduced into the rabbit system by hand, since the ion chamber is not part of the pneumatic transfer system. The decay heat measurement then proceeds in a manner identical to that used for the large foils with two important exceptions: The signal from the ion chamber foil is too small to yield a result with satisfactory statistical precision because of statistical fluctuations in the relatively large ambient background. For this reason the ion chamber measurements are performed with only the plastic scintillator signal on during the "sample in" phases of the measurements. The calibration measurements are performed as for a normal measurement. Since the plastic scintillator is very close to the source and well shielded from background by the liquid scintillator, its signal/background ratio is very high. Secondly, in order to minimize the effect of zero instabilities in the recording system, the electrometer is operated with a sensitivity forty times the normal value. Since this sensitivity would be off scale for the calibration measurement, the calibration is performed at normal sensitivity and then the computer switches to the high sensitivity only when the ion chamber foil is being measured. The exact ratio of the electrometer sensitivities was determined experimentally via an auxiliary computer code which cycled the electrometer between the two sensitivities and averaged the result.

This ion chamber foil measurement yields a precise measure of the response of the plastic scintillator to the fission products of a known number of fissions. We must thus determine the response of the plastic scintillator to the large foils in order to normalize the large foil data. This is accomplished during the course of the large foil measurement by recording a few of the data points with only the plastic scintillator on. These special points provide an overdetermined set of normalizations to the ion chamber foil data.

The measurements of fission rate are routinely repeated for several foils to determine the reproducibility of the normalization. In addition, the gamma-ray lines from the 185 keV ^{235}U or 129 keV ^{239}Pu peaks were measured with a Ge(Li) spectrometer in order to provide additional correlation between the mass of the foil and the measured quantities. In the case of the ^{235}U these correlations were excellent. In the case of the first set of ^{239}Pu foils, the correlations were very poor. Extensive and varied experimental investigations were made in an effort to understand this anomaly, including a repetition of the ^{235}U results. The source of

the problem could not be determined before the last of the 12 ^{239}Pu foils from the first evaporation were destroyed.

The ion chamber foil evaporations were performed by the Isotope Products Division of Oak Ridge National Laboratory (ORNL), and normally require several months to complete. A second set of 16 ^{239}Pu foils was ordered, but in view of the urgency for obtaining a normalized result, a cooperative program was initiated with ORNL to provide an alternative normalization.

3.2 ORNL FISSION RATE

An alternative method of fission rate determination is to do gamma-ray spectrometry on selected fission products whose fission yields and nuclear data are well known. This procedure has been used by other laboratories making decay heat measurements (12, 13).

The procedure developed for the ^{239}Pu measurements at ORNL (12) may be summarized as follows. An ion chamber containing ^{239}Pu was irradiated, and the fission rate was measured via direct counting. After the end of irradiation the line areas of the fission product gamma rays were recorded over a period of many days with a Ge(Li) spectrometer.

One of the large ^{239}Pu foils was irradiated at IRT for 24 hours, and measured in the scintillator in the usual manner. This foil was then shipped to ORNL, where its fission product gamma ray line areas were measured with the same Ge(Li) spectrometer. Several gamma ray lines in the spectra were well separated from interferring lines and could be associated with specific fission products.

Since the decay properties of these isotopes were well known, the relative fission rate in the ORNL ion chamber versus the IRT foil could be calculated. The results of the ORNL measurements are described in Reference 8.

During the course of the ORNL measurements, the second set of evaporated ^{239}Pu foils was completed. The difficulties described in Section 3.1 did not reappear, and the mean value of three determinations of the fission rate were in excellent agreement (0.98%) with the ORNL result. The value used in the present work is an unweighted average of the two results. The fission rates for the 1000 second ^{239}Pu measurements and for all of the uranium measurements were determined exclusively by the IRT ion chamber method.

Section 4

DATA ACQUISITION AND ANALYSIS

4.1 DATA ACQUISTION PROCEDURES

Control of the experiment and data acquisition as well as processing of the measured data are accomplished using a dedicated Hewlett-Packard 2116B computer.

4.1.1 Method of Data Accumulation

Immediately prior to irradiation the signal from the sample is measured in the scintillator in the manner previously described. This preirradiation signal represents the contribution from the natural activity of the sample, fission products from previous irradiations of the sample (if any), and zero signal offset error of the system.

The natural activity of the sample was appreciable only for ^{239}Pu at long cooling times. In some cases a sample was reused after allowing a cooling period of at least seven times the previous irradiation time. The decay heat signal is quite small and decays rather slowly during the course of the next measurement. To account for this decay, an appropriate correction factor for decay was applied to the portion of the background known to be in excess of the natural activity. The correction was calculated from summation calculations of the fission product energy release rates. The zero offset error of the system is primarily due to a small light leakage from the infrared photo-sensor used to detect the presence of the rabbit at the scintillator position. The magnitude of this effect was measured with a rabbit containing no sample.

Following a decay heat measurement the preirradiation signal is subtracted from the decay heat signal, and then the "plastic scintillator only" points are normalized to the plastic scintillator measurements on the ion chambers foils. This normalization is achieved by fitting a second order polynomial to the ion chamber foil data in the immediate cooling time region of interest, and then calculating the magnitude of the curve at the desired time point. This process is repeated for 4 to 6 time points on the cooling curve. The consistancy in the large sample/ion

chamber foil data ratio tends to confirm the validity of background subtractions and/or immunity from fission product leakage.

Since the ^{60}Co sample used to routinely calibrate the system was subject to occasional damage, this working standard was periodically checked against a ^{60}Co source mounted in another rabbit. In both cases sufficient source cover material was used to completely absorb the 300 keV beta activity from ^{60}Co. The energy emission rate was thus based on the energy deposited by the 1173 + 1332 keV gamma rays. The data acquisition code corrects the data for the decay of the source from its birth date. The uncertainty due to the 1.662×10^8 second half life is always small compared to the 1.3% uncertainty in the source intensity at birth.

The signal levels from the ^{239}Pu alloy samples were approximately five times larger than those measured for ^{235}U. At these high levels a small nonlinearity was observed in the scintillator response. The nonlinearity consisted of a 3 to 5% gain increase that occurred over a time span of a few hundred seconds. The effect is probably due to redistribution of active materials within the photomultipliers. In order to eliminate this effect, the neutron flux was reduced an order of magnitude by moving the source. A second set of measurements was made and normalized to the first set in the 3,000-10,000 second cooling time region. These composite data are substantially free of nonlinearity and yet preserve good signal-to-background ratios at long cooling times.

The 35-day ^{235}U irradiations were achieved by use of an auxiliary irradiation position close to the rabbit tube. The neutron flux was measured to be within 3% of that in the main irradiation tube. Two foils were introduced into the auxiliary irradiator 1 and 2 days, respectively, after the rabbit was introduced into the main irradiator. At the end of the 35 days the measurement commenced with the rabbit in the main irradiator, while the foil with one day less irradiation was quickly (~3 minutes) cemented into a rabbit and returned to the main irradiator until its irradiation time expired. An identical procedure was employed for the third foil.

It was not feasible to perform a 35-day ion chamber foil irradiation. Consequently, the number of fissions for the 35-day data was obtained from the 24-hour normalization by the use of a correction factor (13%) obtained from the results of a summation calculation. Thus, the normalization of the 35-day data depends to some extent on the accuracy of the nuclear data library for the long-lived fission

products used in the calculations. These summation calculations were provided by Spinrad at Oregon State University (14).

4.1.2 Decomposition of Beta and Gamma-Ray Components

The measurement procedures described so far yield total decay power. It is also of interest to determine the relative partitioning of this power into beta and gamma ray components. This partitioning also leads to an improvement in accuracy since the corrections for beta and gamma energy loss can be based, at least in part, on measured quantities. With the present measurement system this is possible by repeating the measurements with a beta absorber placed between the sample and the scintillator. For this purpose a 0.163-cm thick iron liner was inserted in the re-entrant hole of the plastic scintillator. The iron absorbs a large fraction of fission product beta energy but only a small fraction of gamma energy. The precise amounts of energy transmitted were calculated as described in subsection 4.2.

The data acquisition code reports the ratio of the net fission product decay signal to the net ^{60}Co standard source signal. The fission product beta and gamma radiations are detected with efficiencies ϵ_β and ϵ_γ, the ^{60}Co radiation is detected with efficiency ϵ_c. Thus, the experimentally measured quantity can be represented as

$$R = \frac{\epsilon_\beta E_\beta + \epsilon_\gamma E_\gamma}{\epsilon_c E_c} , \qquad (4\text{-}1)$$

where E represents the energy release rate of the respective radiation sources. With the iron liner in place, we obtain a new measured quantity

$$R_i = \frac{\epsilon_{\beta i} E_\beta + \epsilon_{\gamma i} E_\gamma}{\epsilon_{ci} E_c} . \qquad (4\text{-}2)$$

The subscript i designates quantities appropriate to the measurement with the iron absorber. It is important to note that the values of $\epsilon_{\gamma i}$ and ϵ_{ci} differ only slightly from the corresponding quantities without the iron, and that the beta transmission ($\epsilon_{\beta i}$) is small. Solving Eqs. 4-1 and 4-2 we obtain the expressions for decomposition of the measured quantities into beta and gamma ray components

$$E_\beta = \frac{E_c \left(R \frac{\epsilon_c}{\epsilon_\gamma} - R_i \frac{\epsilon_{ci}}{\epsilon_{\gamma i}} \right)}{\frac{\epsilon_\beta}{\epsilon_\gamma} - \frac{\epsilon_{\beta i}}{\epsilon_{\gamma i}}} \qquad (4\text{-}3)$$

$$E_\gamma = \frac{R_i \, \epsilon_{ci} \, E_c - \epsilon_{\beta i} \, E_\beta}{\epsilon_{\gamma i}} \, . \qquad (4\text{-}4)$$

4.2 ENERGY LOSS CORRECTIONS

An essential correction to the data is for energy lost through various processes which do not contribute to the measured scintillator signal. These include energy deposition in the structural or other nonactive materials, energy lost in the sample and covers (significant especially for the betas), and radiation so energetic that it passes through the detector without giving up all its energy.

4.2.1 Calculational Procedures

A rather elaborate and sophisticated Monte Carlo program which handles coupled photon-electron transport in three dimensional configurations was applied to this problem (15). In previous work (7), our best estimate of beta and gamma-ray spectra from the literature were used as source spectra. Photons or electrons were sampled from these distributions and the total energy deposited in the active regions was calculated for each source. However, because this is a time consuming and costly process, an alternative procedure was utilized for the present work. The procedure is to define an energy deposition function that relates the energy deposited in active regions of the scintillator to the source energy. This function can be readily determined by the Monte Carlo procedure by selecting monoenergetic photons or electrons and following their transport. By selecting a range of monoenergetic source energies to span the range of interest, an energy deposition function is determined. Separate functions are calculated for betas and gamma rays.

For the present problem there are two different configurations of the scintillator of primary interest - with and without an iron liner between the source and the scintillator. The calculated energy deposition functions for the nuclear calorimeter for gammas and betas with and without the iron liner are shown in Figures 4-1 and 4-2. For the beta case, corrections to the energy deposition

function for different sample configurations were necessary since beta energy losses in the samples and covers are significant. Figure 4-2 shows the iron-out calculation for the normal configuration and for cases where a thicker mylar cover was used, and for the covered ion chamber foil.

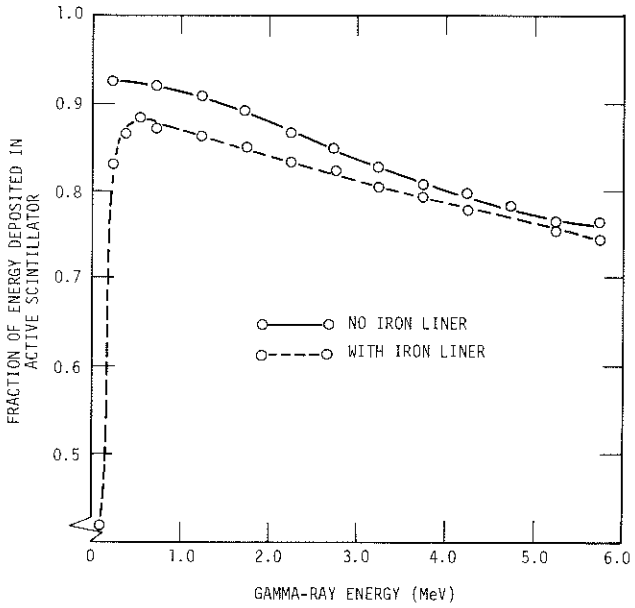

Figure 4-1. Calculated energy deposition in active scintillator for monoenergetic gamma rays

Once the energy deposition function is known for the system, the energy deposited by any source spectra within the range of the function can be easily calculated by

$$E_{dep} = \int_{E_{min}}^{E_{max}} S(E)D(E)dE \quad , \tag{4-5}$$

where S(E) is the source spectrum of betas or gamma rays, and D(E) is the corresponding energy deposition function. The integral is well approximated by a summation, and since D(E) is a smoothly varying function, a second order polynomial interpolation method is used to evaluate D(E) at the energy mesh of S(E).

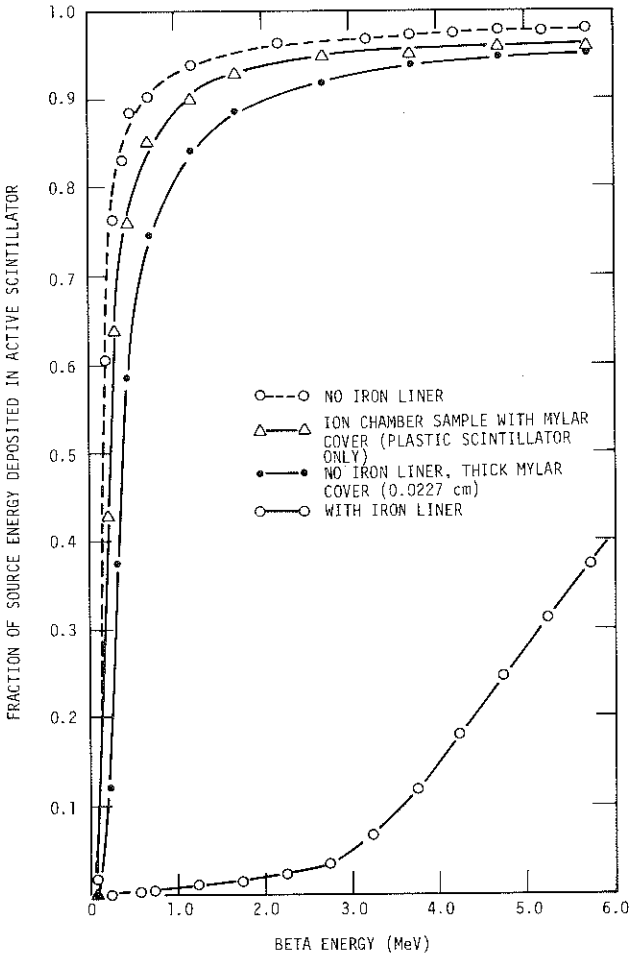

Figure 4-2. Calculated beta energy deposition in active scintillator

4.2.2 Source Spectra

To derive proper correction factors for the present experiments it is necessary to have reasonably good estimates of the beta and gamma-ray spectra from the fission products. Such spectra are cooling time dependent, and hence the corrections must be calculated as a function of cooling time. Since measured spectra for our conditions were not available, use was made of calculated spectra based on the summation method. The procedure is as follows: The build-up and decay of fission products during a prescribed irradiation is calculated using the summation method. The inventory of fission products at each cooling time for which spectra are desired is saved and later folded with spectral data for each of the individual fission products to build up a composite spectrum. This procedure was developed by

England and co-workers (16, 17). A prerequisite for this method is a library of spectra for the individual fission products. Using ENDF/B-IV data (18, 19), England and Stamatelatos rebinned all the available gamma ray data into a uniform group structure, and generated theoretical beta spectra using the end point energies and intensities in the library (20). Spectral data of this type are available for 181 fission product nuclides. Although these represent only a small fraction of the fission products, they are responsible for most of the decay energy, especially at long cooling times. Extensive comparisons with differential decay heat measurements have confirmed the adequacy of the calculational method (21).

Using the methods described, England (22) has calculated beta and gamma-ray spectra for each of the irradiations studied here for both ^{235}U and ^{239}Pu. These spectra have been folded with the energy deposition function of the scintillator to yield corrections for each measurement. The corrections for betas and gamma-rays with and without the iron liner are shown in Figures 4-3 through 4-6.

4.2.3 Corrections to the Data

As may be seen from the figures, the gamma-ray energy loss amounts to 8-11% without the iron liner, and 14-16% with the liner. Small but systematic differences occur for the various irradiation intervals used for the measurements. The accuracy of the correction factors at short (<10 sec) cooling times is limited by the accuracy of the input spectra. However, in the absence of any better estimates the calculated spectra have been used. In any case, it would appear that the correction factor is slowly varying and thus serious errors from the use of the calculated spectra at short times are not expected.

The beta correction factors show a larger variation with cooling time, varying 6-24% depending on irradiation time. When the iron liner is in place, only 1-4% of the beta energy is deposited in the scintillator.

4.3 UNCERTAINTY ANALYSIS

The uncertainties attributed to the measurements are a very important part of the results. The evaluation of various measurements and calculations to develop a new decay heat standard is dependent upon a realistic assessment of errors.

Assessing the uncertainty in the energy loss corrections is difficult. The calculations of the gamma-ray energy loss would seem to be more reliable than the

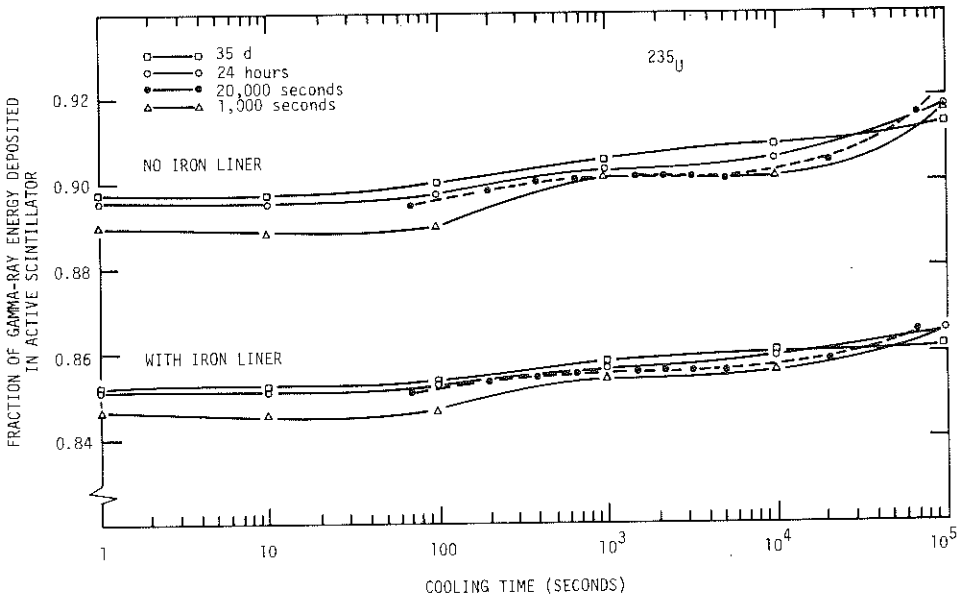

Figure 4-3. Calculated energy loss corrections as a function of cooling time for gamma rays from ^{235}U at the four irradiation times of the measurements.

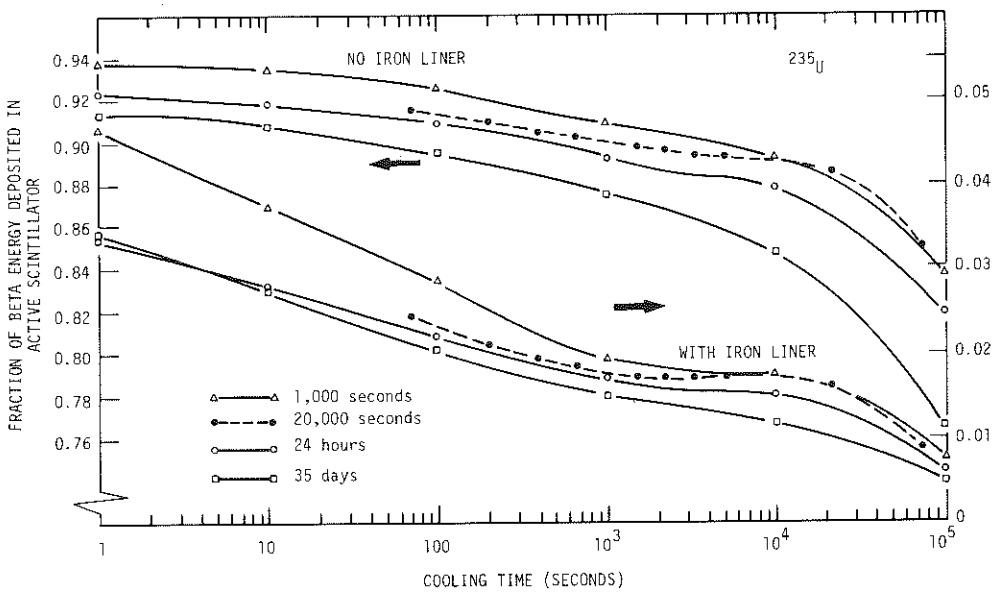

Figure 4-4. Calculated fission product beta energy loss corrections for ^{235}U as a function of cooling time for measured irradiation times

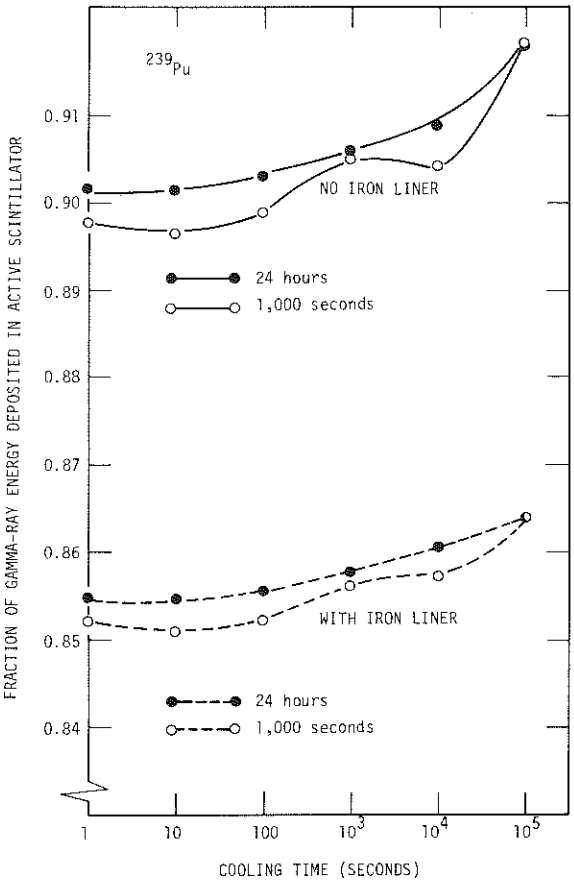

Figure 4-5. Calculated gamma-ray energy loss corrections for ^{239}Pu

beta energy loss corrections. Furthermore, the measurements are made relative to ^{60}Co, and thus gamma energy loss errors tend to cancel. The geometry and composition of the nuclear calorimeter were introduced into the Monte Carlo calculations in considerable detail, and the code itself makes very few approximations. The detailed geometry of the sample construction was also included. The accuracy of the gamma-ray source spectra can be expected to be quite good, especially in the important high energy region of the spectra. At times less than 100 seconds the calculated source spectra have much larger uncertainties due to the limitations of the fission product data library. However, it is not possible to make reliable estimates of the magnitude of this uncertainty. The statistical precision of the Monte Carlo energy deposition calculations for gamma rays is less than 1% for the full energy range. Based on these arguments we assign a 5% uncertainty to the gamma ray energy loss correction.

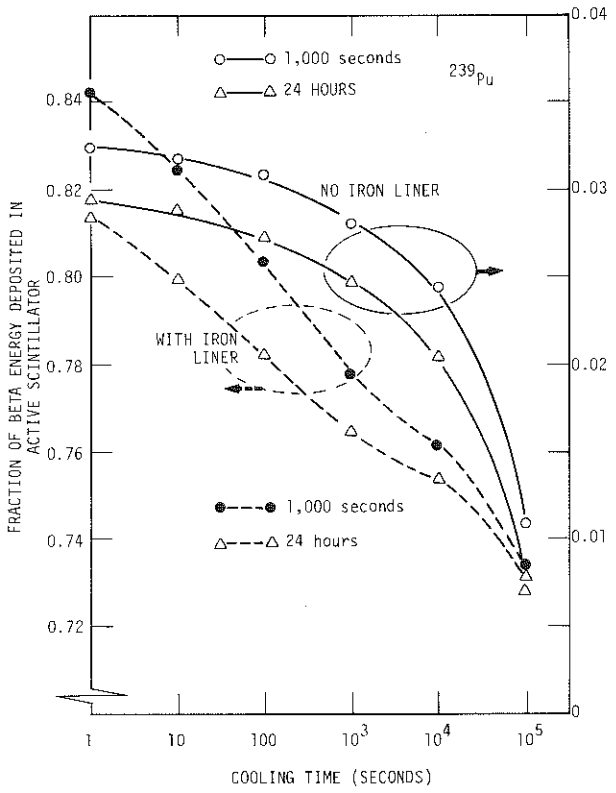

Figure 4-6. Calculated beta energy loss corrections for ^{239}Pu

The beta energy loss correction is considerably less certain. The energy loss mechanisms for betas are much different than those for gamma rays, and also more difficult to accurately calculate. In addition, cancellation of errors relative to the calibration source does not occur for the beta component of decay heat. The statistical precision of the energy loss calculations, especially at low energies, is poorer reaching 5% for 250 keV electrons.

The reliability of the calculated beta spectra is not expected to be as good as for gamma rays. In addition, the nonlinear response of the plastic scintillator at very low energies further degrades the accuracy of the results. For these reasons we assign an uncertainty of 20% to the beta energy loss correction.

In an attempt to verify the beta energy loss corrections calculated by SANDYL, a special decay heat measurement was performed with only the plastic scintillator for ^{235}U after a 24 hour irradiation. In this measurement a mylar cover with a

thickness of 65.58 mg/cm^2 was attached on both sides of the foil for alternate cooling time points. These "covered" points when combined via time interpolation with the "uncovered" points yield an experimental measure of the beta energy absorption in this amount of material. The beta transmission can be obtained at any cooling time from

$$T = R\left(1 + \frac{\epsilon_\gamma E_\gamma}{\epsilon_\beta E_\beta}\right) - \frac{\epsilon_\gamma E_\gamma}{\epsilon_\beta E_\beta} \quad , \tag{4-6}$$

where R is the experimentally measured ratio of the two curves. The value of ϵ_γ for the plastic scintillator is small ($\approx$.25), whereas ϵ_β is near unity. ϵ_β does contain a small correction for the energy loss in the 7 mg/cm^2 permanent cover, although the experimental transmission is not sensitive to this value. The experimental result of 0.6346 at 10,000 seconds cooling is in good agreement with the value of 0.6384 calculated by SANDYL.

An additional source of uncertainty involves the difference in the beta energy loss for the large foils versus the ion chamber foils. The difference in the energy emission rate was calculated with SANDYL to be 5% for ^{235}U and 2% for ^{239}Pu. In view of the additional uncertainty in relative cover thicknesses, an error of 30% is assumed for this correction.

Work is currently in progress at IRT to measure both beta and gamma spectra for ^{239}Pu. As part of this work the nonlinearity of the plastic scintillator material and the beta transmission of the encapsulation material will be measured. This should result in somewhat improved energy loss corrections and a more accurate assessment of the uncertainties.

Another source of error is the balancing of the plastic scintillator with the center section. The accuracy of the balance is limited by statistical fluctuations in the signal to 1.5%. An additional uncertainty involves differences in the gain versus voltage characteristics of the photomultiplier tubes. This increases the balance error to $\approx$2%. This error is systematic to all points in the first 1500 seconds of cooling time, since a rebalancing does not occur in this time region. At later times the balancing error appears as an additional contribution to the random error. Since the plastic scintillator responds primarily to beta particles, the balance error is included only in the beta component of the decay heat.

The uncertainty in the energy emission rate from the ^{60}Co source is 1.3% and after allowance for comparison errors, the calibration accuracy of the working standard is 1.4%.

The error in the fission chamber pulse height extrapolation is assumed to be 25% for the extrapolation. Since the efficiency is typically 96%, the systematic error contribution is 1%.

An additional uncertainty in the normalization involves a small background correction to the ion chamber normalization data. This correction arises from activation of the rabbit assembly. The primary source of the activity is probably due to aluminum rubbed off of the inside of the pneumatic transfer tube. Some of the aluminum can adhere to the part of the rabbit in contact with the tube and produce an appreciable effect relative to the small ion chamber foil signal. The correction is on the order of 2% and a 5% uncertainty is assigned to it.

Section 5

RESULTS AND DISCUSSION

The measured fission product decay heat from ^{239}Pu and ^{235}U for the full measured cooling time range are given in Tables 5-1 through 5-6. The data are expressed in units of MeV/fission. The total decay power and the separate gamma and beta fractions are listed along with the two types of measurement error attributed to the results.

A sensitive way to compare the measured results with the summation calculations is to display the ratio of measured to calculated decay power. For this purpose we used the summation calculations of Spinrad (14) for ^{235}U, and those provided by England (22) for ^{239}Pu. These calculations were done specifically for the irradiation conditions of the experiments with the codes ROPEY (23) and CINDER-10 (24) for ^{235}U and ^{239}Pu, respectively. It should be noted, however, that all of the major summation codes give virtually identical results when used with the same data set. The calculations discussed here use the corrected ENDF/B-IV fission product data library (13, 14).

The resulting ratios for ^{239}Pu and ^{235}U are shown in Figures 5-1 through 5-6. The error bars on the data points represent the random or statistical part of the uncertainty only. Likewise, the uncertainty attributed to the calculated decay heat is not included in the ratio. For those points where no error bars are shown, the statistical uncertainties are as small or smaller than the size of the points.

The characteristic excess of measured over calculated decay power at early cooling times seen in all of the present results has been observed in other recent measurements (12, 13, 25, 26), and is undoubtedly the result of inadequate information in the library (ENDF/B-IV) for short-lived isotopes. This is not surprising considering the heavy reliance on data calculated from nuclear systematics in this time region.

The ^{239}Pu results are consistently higher than the calculations. As might be expected, the agreement tends to be poorest at short cooling times and improves at

Table 5-1

^{239}Pu DECAY HEAT AND EXPERIMENTAL UNCERTAINTIES FOR 1000-SECOND IRRADIATION (UNITS ARE MeV/FISSION, ERRORS ARE IN PERCENT)

PT	TIME SEC	TOTAL	ERROR SYS	ERROR RAND	GAMMA	ERROR SYS	ERROR RAND	BETA	ERROR SYS	ERROR RAND
1	1.06	6.9178	3.7	1.1	3.0289	3.0	1.9	3.8890	4.9	2.4
2	1.31	6.8651	3.7	.9	3.0641	3.0	1.6	3.8010	4.9	2.0
3	1.56	6.7250	3.7	.8	3.0116	3.0	1.6	3.7134	4.9	1.9
4	1.91	6.6464	3.7	.7	2.9412	3.0	1.5	3.7052	4.9	1.7
5	2.31	6.4391	3.7	.7	2.8722	3.0	1.5	3.5669	4.9	1.8
6	2.75	6.2648	3.7	.7	2.8186	3.0	1.5	3.4461	4.9	1.7
7	3.25	6.0960	3.7	.7	2.7051	3.0	1.4	3.3909	4.9	1.7
8	3.81	5.9269	3.7	.6	2.6775	3.0	1.4	3.2493	4.9	1.6
9	4.56	5.7660	3.7	.6	2.5954	3.0	1.4	3.1706	5.0	1.6
10	5.31	5.5323	3.7	.6	2.5393	3.0	1.4	2.9929	5.0	1.6
11	6.20	5.3854	3.7	.6	2.4635	3.0	1.3	2.9219	5.0	1.6
12	7.25	5.2397	3.7	.6	2.3867	3.0	1.3	2.8529	5.0	1.5
13	8.45	5.0710	3.7	.6	2.3212	3.0	1.3	2.7499	5.0	1.5
14	9.86	4.8489	3.7	.6	2.2546	3.0	1.3	2.5943	5.0	1.5
15	11.56	4.6724	3.7	.5	2.1848	3.0	1.3	2.4877	5.0	1.5
16	13.41	4.5004	3.6	.5	2.1225	3.0	1.2	2.3779	5.0	1.5
17	15.56	4.3255	3.6	.5	2.0471	3.0	1.2	2.2784	5.0	1.5
18	18.11	4.1537	3.6	.5	1.9630	3.0	1.2	2.1908	5.0	1.5
19	21.06	3.9767	3.6	.5	1.8856	3.0	1.2	2.0902	5.0	1.5
20	24.41	3.8058	3.6	.5	1.8229	3.0	1.2	1.9829	5.0	1.5
21	28.31	3.6545	3.6	.5	1.7415	3.0	1.2	1.9129	5.0	1.5
22	32.81	3.4693	3.6	.5	1.6703	3.0	1.2	1.7989	5.0	1.5
23	38.00	3.3194	3.6	.5	1.5984	3.0	1.2	1.7210	5.0	1.5
24	44.05	3.1541	3.6	.5	1.5428	3.0	1.2	1.6112	5.0	1.5
25	51.05	2.9882	3.6	.5	1.4613	3.0	1.2	1.5269	5.0	1.5
26	59.16	2.8401	3.6	.5	1.3758	3.0	1.2	1.4643	5.0	1.5
27	68.56	2.6617	3.6	.5	1.3063	3.0	1.2	1.3554	5.0	1.5
28	79.41	2.5108	3.6	.5	1.2236	3.0	1.2	1.2872	5.0	1.5
29	92.05	2.3472	3.6	.5	1.1563	3.0	1.1	1.1909	5.0	1.5
30	106.61	2.2086	3.6	.5	1.0785	3.0	1.2	1.1301	5.0	1.5
31	123.45	2.0628	3.6	.5	1.0127	3.0	1.1	1.0501	5.1	1.5
32	143.00	1.9207	3.6	.5	.9395	3.0	1.2	.9812	5.1	1.5
33	165.66	1.7960	3.6	.5	.8856	3.0	1.2	.9103	5.1	1.6
34	191.95	1.6744	3.6	.5	.8331	3.0	1.2	8412	5.1	1.6
35	260.00	1.4456	3.6	.5	.7252	3.0	1.2	7193	5.1	1.6
36	301.16	1.3440	3.6	.5	.6835	3.0	1.1	.6605	5.1	1.6
37	348.75	1.2472	3.6	.5	.6346	3.0	1.2	.6127	5.1	1.6
38	403.91	1.1576	3.6	.6	.5909	3.0	1.1	.5667	5.1	1.6
39	543.27	.9747	3.6	.6	.5091	3.0	1.2	.4656	5.1	1.8
40	621.95	.9009	3.6	.6	.4788	3.0	1.2	.4302	5.1	1.8
41	700.66	.8297	3.6	.6	.4407	3.0	1.2	.3890	5.1	1.9
42	779.36	.7746	3.6	.6	.4183	3.0	1.2	.3563	5.2	2.0
43	858.06	.7185	3.5	.7	.3950	3.0	1.2	.3236	5.2	2.1
44	936.86	.6761	3.5	.7	.3685	3.0	1.2	.3076	5.2	2.1
45	1015.56	.6398	3.5	.7	.3541	3.0	1.2	.2857	5.2	2.2
46	1094.27	.6004	3.5	.7	.3302	3.0	1.2	.2702	5.2	2.2
47	1253.45	.5302	3.5	.8	.3055	3.0	.6	.2247	5.2	2.0
48	1814.20	.3747	3.4	1.6	.2228	3.0	1.0	.1520	4.8	4.2
49	2049.25	.3252	3.3	1.2	.1991	3.0	.9	.1261	4.8	3.5
50	2540.15	.2554	3.3	1.3	.1601	3.0	1.0	.0953	4.8	3.9
51	2777.60	.2352	3.3	1.3	.1477	3.0	.6	.0874	4.8	3.6
52	3283.60	.1890	3.3	2.0	.1238	3.0	.8	.0652	4.9	6.1
53	4008.05	.1479	3.3	.9	.0957	3.0	1.0	.0522	4.9	3.3
54	4225.15	.1382	3.3	1.8	.0895	3.0	1.2	.0488	4.9	5.5
55	4695.60	.1218	3.3	1.1	.0776	3.0	1.1	.0442	4.9	3.6
56	4947.95	.1116	3.3	1.3	.0726	3.0	.9	.0390	4.9	4.0
57	5503.80	.0973	3.3	1.3	.0645	3.0	.8	0328	4.9	4.1

Table 5-2

^{239}Pu DECAY HEAT AND EXPERIMENTAL UNCERTAINTIES FOR 24-HOUR IRRADIATION (UNITS ARE MeV/FISSION, ERRORS ARE IN PERCENT)

PT	TIME	TOTAL	ERROR		GAMMA	ERROR		BETA	ERROR	
	SEC		SYS	RAND		SYS	RAND		SYS	RAND
1	.05	9.4349	2.8	.7	4.5000	1.8	1.1	4.9349	4.5	1.7
2	1.05	9.4267	2.8	.5	4.5201	1.8	.7	4.9065	4.5	1.2
3	1.35	9.2972	2.8	.5	4.4519	1.8	.7	4.8453	4.5	1.2
4	1.70	9.1260	2.8	.5	4.4019	1.8	.6	4.7241	4.5	1.1
5	2.10	8.9752	2.8	.5	4.2870	1.8	.6	4.6882	4.5	1.1
6	2.55	8.7358	2.7	.5	4.2578	1.8	.6	4.4780	4.5	1.1
7	3.05	8.6173	2.7	.5	4.2041	1.8	.6	4.4132	4.5	1.1
8	3.60	8.4366	2.7	.5	4.1040	1.8	.6	4.3326	4.5	1.1
9	4.35	8.2263	2.7	.5	4.0330	1.8	.5	4.1933	4.5	1.1
10	5.10	8.0509	2.7	.5	3.9681	1.8	.5	4.0828	4.5	1.1
11	6.00	7.9049	2.7	.5	3.8963	1.8	.5	4.0086	4.5	1.1
12	7.05	7.7180	2.7	.5	3.8133	1.8	.5	3.9047	4.5	1.1
13	8.25	7.5309	2.7	.5	3.7552	1.8	.5	3.7756	4.5	1.1
14	9.65	7.3510	2.7	.5	3.6731	1.8	.5	3.6780	4.5	1.0
15	11.25	7.1854	2.7	.5	3.6086	1.8	.5	3.5768	4.5	1.0
16	13.15	6.9598	2.7	.5	3.5307	1.8	.5	3.4291	4.5	1.1
17	15.35	6.7883	2.7	.5	3.4599	1.8	.5	3.3284	4.5	1.1
18	17.85	6.6281	2.7	.5	3.4019	1.8	.4	3.2262	4.5	1.1
19	20.75	6.4402	2.7	.5	3.3234	1.8	.4	3.1168	4.5	1.1
20	24.10	6.2673	2.7	.5	3.2503	1.8	.4	3.0170	4.6	1.1
21	27.95	6.0871	2.7	.5	3.1700	1.8	.4	2.9172	4.6	1.1
22	32.40	5.9352	2.7	.5	3.0898	1.8	.5	2.8454	4.6	1.1
23	37.65	5.7709	2.7	.5	3.0120	1.8	.4	2.7589	4.6	1.1
24	43.65	5.5933	2.7	.5	2.9382	1.8	.5	2.6551	4.6	1.1
25	50.65	5.4282	2.7	.5	2.8531	1.8	.5	2.5750	4.6	1.1
26	58.75	5.2527	2.7	.5	2.7725	1.8	.5	2.4802	4.6	1.1
27	68.15	5.0849	2.6	.5	2.7025	1.8	.5	2.3824	4.6	1.1
28	79.05	4.9220	2.7	.5	2.6063	1.8	.5	2.3157	4.6	1.1
29	91.65	4.7506	2.7	.5	2.5283	1.8	.5	2.2223	4.6	1.2
30	106.30	4.6034	2.7	.5	2.4565	1.8	.5	2.1469	4.6	1.2
31	123.20	4.4403	2.6	.5	2.3821	1.8	.5	2.0583	4.6	1.2
32	142.85	4.2959	2.6	.5	2.3024	1.8	.5	1.9935	4.6	1.2
33	165.55	4.1467	2.6	.5	2.2364	1.8	.5	1.9103	4.6	1.2
34	191.85	4.0032	2.6	.5	2.1698	1.8	.5	1.8335	4.7	1.2
35	259.50	3.7293	2.6	.5	2.0287	1.8	.5	1.7005	4.7	1.3
36	300.40	3.5969	2.6	.5	1.9659	1.8	.5	1.6300	4.7	1.3
37	347.80	3.4656	2.6	.5	1.9078	1.8	.5	1.5578	4.7	1.3
38	402.65	3.3390	2.6	.5	1.8370	1.8	.6	1.5021	4.7	1.4
39	542.00	3.0734	2.6	.6	1.7057	1.8	.6	1.3677	4.7	1.4
40	620.35	2.9521	2.6	.6	1.6470	1.8	.6	1.3051	4.7	1.5
41	698.75	2.8398	2.6	.6	1.5891	1.8	.6	1.2507	4.8	1.5
42	777.05	2.7405	2.6	.6	1.5387	1.8	.6	1.2018	4.8	1.6
43	855.35	2.6553	2.6	.6	1.4876	1.8	.7	1.1676	4.8	1.6
44	933.65	2.5762	2.6	.6	1.4441	1.8	.7	1.1321	4.8	1.6
45	1011.95	2.4998	2.6	.6	1.4054	1.8	.7	1.0934	4.8	1.6
46	1090.25	2.4241	2.6	.6	1.3684	1.8	.7	1.0558	4.8	1.7
47	1249.30	2.2976	2.6	.6	1.2971	1.8	1.1	1.0005	4.8	2.1
48	2542.15	1.6274	2.5	1.5	.9365	1.8	.4	.6909	4.4	3.6
49	2751.50	1.5844	2.5	1.2	.8972	1.8	.4	.6872	4.4	2.8
50	3234.40	1.4372	2.5	1.4	.8169	1.8	1.1	.6203	4.5	3.5
51	4169.20	1.2576	2.5	1.4	.7054	1.8	.8	.5512	4.5	3.4
52	4637.00	1.1909	2.5	1.4	.6706	1.8	.7	.5202	4.5	3.3
53	4859.80	1.1592	2.5	1.4	.6489	1.8	.7	.5103	4.5	3.4
54	5326.60	1.0960	2.5	1.4	.6086	1.8	.7	.4874	4.5	3.2
55	5951.00	1.0023	2.5	1.3	.5640	1.8	.6	.4383	4.6	3.1
56	7988.70	.8685	2.6	1.4	.4637	1.8	.7	.4048	4.6	3.1
57	8988.40	.8153	2.7	1.4	.4331	1.8	.6	.3822	4.7	3.0
58	10014.40	.7593	2.7	1.4	.3971	1.8	.8	.3622	4.7	3.1
59	11028.30	.7216	2.7	1.4	.3737	1.8	.6	.3479	4.7	3.0
60	14502.50	.6123	2.8	1.4	.3066	1.8	.5	.3057	4.8	2.9
61	17077.60	.5541	2.8	1.4	.2749	1.8	.5	.2792	4.8	2.9
62	19653.80	.5053	2.8	1.4	.2511	1.8	.3	.2543	4.8	2.9
63	22251.30	.4669	2.9	1.4	.2280	1.8	.3	.2389	4.8	2.8
64	24832.00	.4335	2.9	1.4	.2113	1.8	.3	.2223	4.9	2.8
65	27409.20	.4060	2.9	1.4	.1981	1.8	.3	.2079	4.9	2.8
66	32006.60	.3654	2.9	1.4	.1779	1.8	.3	.1875	4.9	2.8
67	37024.70	.3265	2.9	1.4	.1609	1.8	.3	.1656	5.0	2.8
68	42029.70	.2956	3.0	1.4	.1459	1.8	.3	.1497	5.1	2.8
69	47025.90	.2708	3.0	1.4	.1338	1.8	.3	.1371	5.1	2.8
70	54958.50	.2040	3.0	1.4	.1039	1.8	.4	.1001	5.3	2.9
71	74953.50	.1778	3.0	1.4	.0911	1.8	.3	.0867	5.4	2.9
72	94948.20	.1400	3.1	1.4	.0733	1.8	.4	.0667	5.6	3.0
73	104968.00	.1265	3.1	1.4	.0669	1.8	.3	.0596	5.7	3.0
74	129967.00	.1008	3.0	1.4	.0543	1.8	.4	.0466	5.7	3.0

Table 5-3

^{235}U DECAY HEAT AND EXPERIMENTAL UNCERTAINTIES FOR 1000-SECOND IRRADIATION (UNITS ARE MeV/FISSION, ERRORS ARE IN PERCENT)

PT	TIME SEC	TOTAL	ERROR SYS	ERROR RAND	GAMMA	ERROR SYS	ERROR RAND	BETA	ERROR SYS	ERROR RAND
1	1.85	8.4428	3.1	.3	4.2337	2.9	.7	4.2092	3.7	.9
2	1.35	8.2162	3.1	.3	3.9275	2.9	.8	4.2887	3.7	.9
3	1.70	8.0232	3.1	.3	3.8150	2.9	.7	4.2082	3.7	.9
4	2.10	7.7760	3.1	.3	3.7127	2.9	.7	4.0632	3.7	.9
5	2.50	7.6129	3.1	.3	3.6436	2.9	.8	3.9693	3.7	.9
6	3.05	7.3776	3.1	.3	3.5567	2.9	.7	3.8209	3.7	.9
7	3.60	7.1322	3.1	.3	3.4815	2.9	.8	3.6507	3.7	.9
8	4.25	6.9178	3.1	.3	3.4054	2.9	.8	3.5124	3.7	.9
9	5.10	6.6658	3.1	.3	3.2959	2.9	.7	3.3691	3.7	.9
10	6.00	6.4539	3.1	.3	3.1931	2.9	.7	3.2608	3.7	.9
11	7.05	6.2096	3.1	.3	3.0863	2.9	.8	3.1233	3.7	1.0
12	8.25	5.9557	3.1	.3	3.0062	2.9	.8	2.9496	3.7	1.0
13	9.65	5.7563	3.1	.3	2.9057	2.9	.8	2.8506	3.7	1.0
14	11.25	5.5248	3.1	.3	2.8104	2.9	.8	2.7144	3.7	1.0
15	13.10	5.2804	3.1	.3	2.6950	2.9	.8	2.5854	3.7	1.0
16	15.25	5.0489	3.1	.3	2.5993	2.9	.8	2.4497	3.7	1.1
17	17.75	4.8332	3.1	.3	2.5028	2.9	.8	2.3304	3.7	1.1
18	20.65	4.6243	3.1	.3	2.3958	2.9	.8	2.2286	3.7	1.1
19	24.00	4.4107	3.1	.3	2.2946	2.9	.8	2.1161	3.7	1.1
20	27.90	4.1869	3.1	.3	2.2016	2.9	.8	1.9853	3.7	1.2
21	32.40	3.9981	3.1	.4	2.0969	2.9	.8	1.9012	3.7	1.2
22	37.60	3.7871	3.1	.4	2.0084	2.9	.8	1.7787	3.7	1.2
23	43.75	3.5795	3.1	.4	1.8894	2.9	.8	1.6901	3.7	1.2
24	50.75	3.3904	3.1	.4	1.7928	2.9	.8	1.5976	3.8	1.2
25	58.85	3.1809	3.1	.4	1.6849	2.9	.9	1.4960	3.8	1.3
26	68.25	2.9889	3.1	.4	1.5893	2.9	.9	1.3996	3.8	1.3
27	79.15	2.8025	3.1	.4	1.4889	2.9	.9	1.3136	3.8	1.3
28	91.80	2.6135	3.1	.4	1.3948	2.9	.9	1.2187	3.8	1.4
29	106.45	2.4384	3.1	.4	1.2977	2.9	.9	1.1407	3.8	1.4
30	123.35	2.2640	3.1	.5	1.1965	2.9	.9	1.0675	3.8	1.4
31	143.00	2.0974	3.1	.5	1.1084	2.9	.9	.9890	3.8	1.5
32	165.65	1.9369	3.1	.5	1.0285	2.9	1.0	.9084	3.8	1.5
33	191.95	1.7973	3.1	.5	.9455	2.9	1.0	.8518	3.8	1.5
34	259.80	1.5231	3.1	.6	.8010	2.9	1.0	.7221	3.8	1.6
35	300.60	1.4067	3.1	.6	.7411	2.9	1.1	.6656	3.8	1.7
36	347.85	1.2928	3.1	.6	.6835	2.9	1.1	.6093	3.8	1.8
37	402.60	1.1853	3.1	.6	.6258	2.9	1.1	.5595	3.8	1.9
38	541.90	.9900	3.1	.7	.5274	2.9	1.1	.4627	3.9	2.0
39	620.70	.9103	3.1	.8	.4829	2.9	1.2	.4273	3.9	2.1
40	699.50	.8407	3.1	.8	.4508	2.9	1.2	.3900	3.9	2.2
41	778.40	.7816	3.1	.8	.4188	2.9	1.2	.3628	3.9	2.3
42	857.20	.7311	3.1	.9	.3902	2.9	1.3	.3409	3.9	2.4
43	936.00	.6860	3.1	.9	.3692	2.9	1.3	.3168	3.9	2.5
44	1014.80	.6448	3.1	.9	.3507	2.9	1.3	.2942	3.9	2.6
45	1093.60	.6098	3.1	1.0	.3308	2.9	1.3	.2790	3.9	2.7
46	1252.95	.5496	3.1	1.1	.2989	2.9	1.1	.2508	3.9	2.6
47	1812.80	.3903	3.0	1.4	.2093	2.9	1.2	.1810	3.4	3.4
48	2038.35	.3494	3.0	1.5	.1904	2.9	1.7	.1591	3.4	3.9
49	2524.30	.2762	3.0	1.4	.1548	2.9	2.1	.1213	3.4	4.1
50	2738.75	.2620	3.0	1.2	.1436	2.9	1.4	.1184	3.4	3.2
51	3208.65	.2110	3.0	1.4	.1232	2.9	1.9	.0878	3.4	4.2
52	3899.75	.1741	3.0	1.5	.1005	2.9	2.4	.0736	3.4	4.9
53	4115.95	.1587	3.0	1.6	.0952	2.9	4.2	.0635	3.4	7.5
54	4602.50	.1356	3.0	1.9	.0848	2.9	3.9	.0508	3.5	8.3
55	4822.40	.1332	3.0	2.8	.0799	2.9	3.4	.0533	3.5	8.6
56	5324.00	.1181	3.0	2.2	.0689	2.9	1.7	.0492	3.5	5.7
57	5970.00	.1011	3.0	1.6	.0612	2.9	2.6	.0399	3.5	5.6
58	8007.20	.0725	3.0	1.7	.0412	2.9	3.7	.0313	3.5	6.3
59	9003.25	.0619	3.0	2.3	.0346	2.9	3.9	.0272	3.5	7.2
60	10016.70	.0556	3.0	2.6	.0321	2.9	4.3	.0235	3.6	8.5
61	11000.00	.0492	3.0	3.0	.0278	2.9	4.2	.0214	3.6	8.8
62	14506.70	.0327	3.1	2.1	.0178	2.9	5.6	.0157	3.6	7.5
63	17075.85	.0267	3.1	2.3	.0138	2.9	6.3	.0129	3.6	8.4
64	19658.90	.0215	3.1	3.5	.0101	2.9	9.0	.0114	3.6	10.3
65	22248.00	.0181	3.1	4.5	.0088	2.9	9.6	.0093	3.6	12.6
66	24859.55	.0163	3.1	4.6	.0079	2.9	10.6	.0084	3.6	13.4
67	27452.35	.0154	3.1	4.2	.0073	2.9	12.1	.0082	3.6	13.4
68	32110.75	.0114	3.0	6.3	.0072	2.9	13.2	.0041	3.6	29.0
69	37023.05	.0104	3.1	6.4	.0055	2.9	15.7	.0049	3.6	22.0
70	42069.45	.0080	3.0	8.5	.0047	2.9	20.0	.0034	3.6	24.4
71	47060.15	.0077	3.3	8.4	.0028	2.9	41.2	.0058	3.6	18.1
72	52092.76	.0067	3.3	8.8	.0019	2.9	44.7	.0048	3.6	21.4

Table 5-4

^{235}U DECAY HEAT AND EXPERIMENTAL UNCERTAINTIES FOR 20,000-SECOND IRRADIATION (UNITS ARE MeV/FISSION, ERRORS ARE IN PERCENT)

PT	TIME SEC	TOTAL	ERROR SYS	ERROR RAND	GAMMA	ERROR SYS	ERROR RAND	BETA	ERROR SYS	ERROR RAND
1	.95	11.0345	3.2	.4	5.5572	2.9	.8	5.4774	3.9	1.2
2	1.25	10.9029	3.1	.4	5.5729	2.9	.8	5.3300	3.9	1.2
3	1.59	10.6504	3.1	.4	5.4210	2.9	.8	5.2294	3.9	1.2
4	2.00	10.3939	3.1	.4	5.2906	2.9	.8	5.1033	3.9	1.2
5	2.44	10.1775	3.1	.4	5.2076	2.9	.8	4.9698	3.9	1.2
6	2.94	9.9514	3.1	.4	5.1005	2.9	.8	4.8438	3.9	1.2
7	3.50	9.6926	3.1	.4	5.0127	2.9	.8	4.6799	3.9	1.2
8	4.25	9.4443	3.1	.4	4.8735	2.9	.8	4.5708	3.9	1.2
9	5.00	9.2100	3.1	.4	4.7917	2.9	.8	4.4183	3.9	1.2
10	5.89	8.9577	3.1	.4	4.7035	2.9	.5	4.2543	3.9	1.0
11	6.95	8.6960	3.1	.4	4.5557	2.9	.5	4.1403	3.9	1.0
12	8.16	8.4483	3.1	.4	4.4452	2.9	.5	4.0031	3.9	1.1
13	9.55	8.2052	3.1	.4	4.3325	2.9	.5	3.8727	3.9	1.1
14	11.16	7.9706	3.1	.4	4.2322	2.9	.5	3.7384	3.9	1.1
15	13.05	7.7218	3.1	.4	4.1140	2.9	.5	3.6078	3.9	1.1
16	15.25	7.4903	3.1	.4	4.0079	2.9	.5	3.4824	3.9	1.1
17	17.70	7.2573	3.1	.4	3.9155	2.9	.5	3.3418	3.9	1.1
18	20.64	7.0320	3.1	.4	3.8047	2.9	.5	3.2273	3.9	1.1
19	24.00	6.7951	3.1	.4	3.6858	2.9	.5	3.1093	3.9	1.1
20	27.84	6.5817	3.1	.5	3.5858	2.9	.5	2.9960	3.9	1.1
21	32.30	6.3653	3.1	.5	3.4753	2.9	.5	2.8980	3.9	1.2
22	37.55	6.1483	3.1	.5	3.3597	2.9	.5	2.7886	3.9	1.2
23	43.55	5.9281	3.1	.5	3.2438	2.9	.5	2.6843	3.9	1.2
24	50.55	5.7200	3.1	.5	3.1341	2.9	.5	2.5859	3.9	1.2
25	58.59	5.5153	3.1	.5	3.0239	2.9	.5	2.4914	3.9	1.2
26	67.95	5.3078	3.1	.5	2.9143	2.9	.5	2.3935	3.9	1.2
27	78.80	5.0972	3.1	.5	2.8052	2.9	.5	2.2920	3.9	1.2
28	91.34	4.9002	3.1	.5	2.6965	2.9	.5	2.2037	3.9	1.2
29	105.89	4.6992	3.1	.5	2.5908	2.9	.5	2.1084	3.9	1.2
30	122.75	4.5029	3.1	.5	2.4847	2.9	.5	2.0182	3.9	1.3
31	142.30	4.3117	3.1	.5	2.3826	2.9	.5	1.9291	3.9	1.3
32	165.00	4.1358	3.1	.5	2.2848	2.9	.5	1.8510	3.9	1.3
33	191.41	3.9673	3.1	.5	2.1909	2.9	.5	1.7764	3.9	1.3
34	259.14	3.6318	3.1	.5	2.0083	2.9	.6	1.6227	3.9	1.4
35	300.14	3.4808	3.1	.5	1.9287	2.9	.6	1.5541	4.0	1.4
36	347.55	3.3298	3.1	.5	1.8483	2.9	.6	1.4815	4.0	1.4
37	402.45	3.1841	3.1	.5	1.7703	2.9	.6	1.4139	4.0	1.4
38	541.09	2.8985	3.1	.5	1.6137	2.9	.6	1.2848	4.0	1.5
39	619.59	2.7690	3.1	.5	1.5437	2.9	.6	1.2253	4.0	1.5
40	698.00	2.6557	3.1	.6	1.4842	2.9	.6	1.1715	4.0	1.5
41	776.39	2.5532	3.1	.6	1.4297	2.9	.7	1.1235	4.0	1.5
42	854.80	2.4605	3.1	.6	1.3808	2.9	.7	1.0797	4.0	1.5
43	933.20	2.3805	3.1	.6	1.3340	2.9	.7	1.0465	4.0	1.6
44	1011.55	2.3012	3.1	.6	1.2956	2.9	.7	1.0056	4.0	1.6
45	1089.84	2.2291	3.1	.6	1.2567	2.9	.7	.9725	4.0	1.6
46	1249.05	2.1006	3.1	.5	1.1867	2.9	.7	.9139	4.0	1.5
47	1796.50	1.7371	3.0	1.0	.9949	2.9	.6	.7421	3.5	2.6
48	2012.95	1.6287	3.0	1.3	.9305	2.9	.6	.6982	3.5	3.1
49	2472.00	1.4474	3.0	1.0	.8315	2.9	.6	.6159	3.5	2.4
50	2687.20	1.3649	3.0	1.1	.7879	2.9	.6	.5770	3.5	2.8
51	3162.55	1.2358	3.0	1.1	.7112	2.9	.7	.5247	3.6	2.7
52	3862.09	1.0993	3.0	1.0	.6311	2.9	.9	.4682	3.6	2.5
53	4079.30	1.0545	3.0	.9	.6087	2.9	.7	.4538	3.6	2.4
54	4559.34	.9686	3.0	1.3	.5556	2.9	1.1	.4130	3.6	3.3
55	4776.95	.9361	3.0	1.2	.5377	2.9	1.1	.3984	3.6	3.1
56	5259.30	.8855	3.0	1.0	.4954	2.9	.4	.3891	3.6	2.4
57	5862.50	.8183	3.0	1.0	.4525	2.9	.4	.3657	3.6	2.2
58	7816.20	.6499	3.0	1.0	.3538	2.9	.5	.2961	3.6	2.2
59	8804.00	.5949	3.0	1.0	.3179	2.9	.5	.2770	3.6	2.2
60	9778.20	.5423	3.1	1.0	.2859	2.9	.6	.2564	3.6	2.3
61	10777.41	.5052	3.1	1.0	.2597	2.9	.5	.2455	3.6	2.2
62	11754.50	.4647	3.1	1.1	.2365	2.9	.5	.2282	3.6	2.2
63	14476.05	.3854	3.1	1.1	.1874	2.9	.6	.1980	3.6	2.2
64	17018.20	.3332	3.1	1.1	.1573	2.9	.7	.1759	3.6	2.2
65	19586.19	.2905	3.1	1.1	.1335	2.9	.8	.1570	3.6	2.2
66	22130.30	.2590	3.1	1.2	.1155	2.9	.8	.1435	3.7	2.3
67	24674.09	.2353	3.1	1.2	.1038	2.9	1.1	.1315	3.7	2.4
68	27218.95	.2135	3.2	1.2	.0939	2.9	1.1	.1196	3.7	2.3
69	31978.55	.1794	3.2	1.2	.0791	2.9	1.3	.1003	3.7	2.5
70	37004.44	.1547	3.2	1.3	.0680	2.9	1.4	.0867	3.8	2.5
71	41979.81	.1356	3.2	1.3	.0591	2.9	1.6	.0765	3.8	2.6
72	46992.84	.1182	3.2	1.3	.0502	2.9	2.1	.0680	3.9	2.8
73	52007.31	.1069	3.3	1.4	.0450	2.9	2.1	.0619	3.9	2.8
74	64933.41	.0791	3.3	1.4	.0365	2.9	2.6	.0425	4.1	3.4
75	74947.69	.0659	3.3	1.6	.0306	2.9	2.6	.0353	4.1	3.8
76	94942.84	.0485	3.3	1.9	.0238	2.9	3.4	.0247	4.1	4.9
77	104933.81	.0416	3.2	1.8	.0213	2.9	3.8	.0202	4.1	5.5

Table 5-5

^{235}U DECAY HEAT AND EXPERIMENTAL UNCERTAINTIES FOR 24-HOUR IRRADIATION (UNITS ARE MeV/FISSION, ERRORS ARE IN PERCENT)

PT	TIME SEC	TOTAL	ERROR SYS	ERROR RAND	GAMMA	ERROR SYS	ERROR RAND	BETA	ERROR SYS	ERROR RAND
1	.05	11.7559	3.1	.8	6.0556	2.9	.8	5.7002	3.8	1.9
2	1.05	11.6298	3.1	.6	5.9676	2.9	.8	5.6622	3.8	1.5
3	1.35	11.4759	3.1	.6	5.8330	2.9	.8	5.6430	3.8	1.4
4	1.70	11.2331	3.1	.5	5.7740	2.9	.8	5.4583	3.8	1.4
5	2.10	11.0160	3.1	.5	5.6888	2.9	.8	5.3272	3.8	1.4
6	2.55	10.8643	3.1	.5	5.5967	2.9	.7	5.2676	3.8	1.3
7	3.05	10.5348	3.1	.5	5.5080	2.9	.7	5.0269	3.8	1.3
8	3.60	10.3065	3.1	.5	5.3810	2.9	.7	4.9255	3.8	1.3
9	4.30	10.0371	3.1	.5	5.3046	2.9	.7	4.7325	3.8	1.2
10	5.10	9.8274	3.1	.5	5.1878	2.9	.6	4.6396	3.8	1.2
11	6.00	9.6028	3.1	.4	5.0509	2.9	.6	4.5519	3.8	1.2
12	7.05	9.3190	3.1	.4	4.9659	2.9	.6	4.3531	3.8	1.2
13	8.25	9.0799	3.1	.4	4.8393	2.9	.6	4.2406	3.8	1.1
14	9.65	8.8672	3.1	.4	4.7328	2.9	.6	4.1344	3.8	1.1
15	11.25	8.5930	3.1	.4	4.6552	2.9	.6	3.9377	3.9	1.1
16	13.10	8.3566	3.1	.4	4.5153	2.9	.6	3.8413	3.9	1.1
17	15.25	8.1314	3.1	.4	4.3956	2.9	.6	3.7358	3.9	1.1
18	17.80	7.8848	3.1	.4	4.3051	2.9	.5	3.5796	3.9	1.1
19	20.65	7.6593	3.1	.4	4.2026	2.9	.5	3.4567	3.9	1.1
20	24.00	7.4255	3.1	.4	4.1052	2.9	.6	3.3202	3.9	1.1
21	27.90	7.2026	3.1	.4	3.9849	2.9	.5	3.2177	3.9	1.1
22	32.40	7.0051	3.1	.4	3.8580	2.9	.5	3.1471	3.9	1.1
23	37.55	6.7794	3.1	.4	3.7435	2.9	.5	3.0359	3.9	1.1
24	43.60	6.5536	3.1	.4	3.6301	2.9	.5	2.9235	3.9	1.1
25	50.55	6.3435	3.1	.4	3.5262	2.9	.5	2.8173	3.9	1.1
26	58.60	6.1381	3.1	.4	3.4196	2.9	.5	2.7186	3.9	1.1
27	68.00	5.9281	3.1	.4	3.3022	2.9	.5	2.6259	3.9	1.1
28	78.95	5.7192	3.1	.4	3.1854	2.9	.5	2.5339	3.9	1.1
29	91.55	5.5154	3.1	.4	3.0609	2.9	.5	2.4546	3.9	1.1
30	106.15	5.3023	3.1	.4	2.9577	2.9	.5	2.3446	3.9	1.1
31	123.15	5.1200	3.1	.4	2.8538	2.9	.5	2.2662	3.9	1.1
32	142.75	4.9283	3.1	.4	2.7385	2.9	.5	2.1897	3.9	1.1
33	165.50	4.7411	3.1	.4	2.6360	2.9	.5	2.1052	3.9	1.1
34	191.80	4.5746	3.1	.4	2.5370	2.9	.5	2.0376	4.0	1.0
35	259.50	4.2329	3.1	.4	2.3541	2.9	.5	1.8788	4.0	1.1
36	300.40	4.0763	3.1	.4	2.2615	2.9	.5	1.8148	4.0	1.1
37	347.80	3.9273	3.1	.4	2.1786	2.9	.5	1.7487	4.0	1.1
38	402.65	3.7835	3.1	.4	2.0944	2.9	.5	1.6891	4.0	1.1
39	541.30	3.4948	3.1	.4	1.9338	2.9	.5	1.5610	4.0	1.1
40	619.65	3.3564	3.1	.4	1.8608	2.9	.5	1.4956	4.0	1.1
41	698.00	3.2382	3.1	.4	1.7982	2.9	.5	1.4400	4.0	1.1
42	776.35	3.1409	3.1	.4	1.7423	2.9	.6	1.3986	4.1	1.1
43	854.60	3.0403	3.1	.4	1.6898	2.9	.6	1.3506	4.1	1.1
44	932.90	2.9569	3.2	.4	1.6382	2.9	.6	1.3187	4.1	1.1
45	1011.20	2.8721	3.2	.8	1.5972	2.9	.6	1.2749	4.1	.7
46	1089.50	2.7994	3.2	.4	1.5560	2.9	.6	1.2434	4.1	1.1
47	1248.58	2.6596	3.2	.4	1.4789	2.9	.6	1.1808	4.1	1.1
48	1783.00	2.2760	3.0	1.2	1.2761	2.9	1.1	.9998	3.6	3.1
49	1986.10	2.1933	3.0	1.0	1.2103	2.9	1.0	.9750	3.6	2.6
50	2436.60	2.0296	3.0	1.3	1.0909	2.9	.6	.9387	3.6	2.9
51	2632.70	1.9270	3.0	1.2	1.0478	2.9	.8	.8792	3.6	2.7
52	3081.60	1.8055	3.0	1.1	.9793	2.9	1.1	.8262	3.6	2.8
53	3728.80	1.6359	3.0	1.0	.8987	2.9	1.2	.7372	3.6	2.6
54	3923.70	1.6185	3.0	1.6	.8796	2.9	1.2	.7389	3.6	3.9
55	4398.50	1.4837	3.0	1.3	.8259	2.9	1.0	.6577	3.6	3.2
56	4599.80	1.4735	3.1	1.3	.8018	2.9	1.1	.6717	3.6	3.1
57	5040.20	1.4016	3.1	1.6	.7609	2.9	.7	.6407	3.6	3.7
58	5587.80	1.3361	3.1	1.0	.7104	2.9	.5	.6258	3.7	2.3
59	6530.60	1.2230	3.1	1.1	.6379	2.9	.6	.5851	3.7	2.3
60	8397.90	1.0625	3.1	1.1	.5341	2.9	.7	.5283	3.7	2.3
61	9323.60	.9814	3.1	1.1	.4994	2.9	.7	.4820	3.7	2.4
62	10282.20	.9453	3.1	1.1	.4666	2.9	.7	.4706	3.7	2.2
63	11232.40	.9027	3.1	1.1	.4380	2.9	.6	.4646	3.8	2.2
64	14448.70	.7604	3.1	1.1	.3630	2.9	.6	.3975	3.8	2.2
65	16920.80	.6860	3.2	1.1	.3219	2.9	.7	.3642	3.8	2.2
66	19425.00	.6211	3.2	1.1	.2924	2.9	.6	.3287	3.8	2.2
67	21959.10	.5732	3.2	1.1	.2660	2.9	.6	.3071	3.8	2.2
68	24467.50	.5201	3.2	1.1	.2450	2.9	.5	.2831	3.9	2.2
69	26947.80	.4909	3.2	1.1	.2274	2.9	.6	.2635	3.9	2.2
70	31920.30	.4351	3.2	1.1	.2034	2.9	.7	.2317	3.9	2.2
71	36942.40	.3824	3.2	1.1	.1799	2.9	.9	.2025	4.0	2.3
72	41949.70	.3406	3.2	1.2	.1617	2.9	.9	.1789	4.0	2.3
73	46932.70	.3084	3.2	1.1	.1501	2.9	1.1	.1583	4.1	2.4
74	51935.20	.2817	3.2	1.1	.1387	2.9	1.0	.1430	4.1	2.4
75	64986.60	.2259	3.3	1.1	.1143	2.9	1.1	.1116	4.2	2.5
76	74896.00	.1916	3.3	1.1	.0991	2.9	1.3	.0925	4.3	2.7
77	94923.59	.1491	3.3	1.2	.0792	2.9	1.5	.0699	4.6	3.1
78	100803.50	.1412	3.3	1.3	.0736	2.9	1.4	.0676	4.6	3.2
79	106580.00	.1302	3.3	1.3	.0698	2.9	1.9	.0611	4.6	3.5
80	129893.00	.1025	3.3	1.4	.0574	2.9	2.2	.0451	4.6	4.3
81	154877.59	.0850	3.3	1.8	.0466	2.9	2.7	.0384	4.6	5.1

Table 5-6

^{235}U DECAY HEAT AND EXPERIMENTAL UNCERTAINTIES FOR 35-DAY IRRADIATION (UNITS ARE MeV/FISSION, ERRORS ARE IN PERCENT)

PT	TIME SEC	TOTAL	ERROR SYS	ERROR RAND	GAMMA	ERROR SYS	ERROR RAND	BETA	ERROR SYS	ERROR RAND
1	1.30	12.1006	3.1	.8	6.5526	2.9	.9	5.6280	3.9	2.0
2	1.50	12.0488	3.1	.8	6.5387	2.9	.9	5.5101	3.9	2.0
3	1.75	11.9211	3.1	.8	6.4843	2.9	.9	5.4367	3.9	2.0
4	2.15	11.7087	3.1	.8	6.3200	2.9	.9	5.3886	3.9	2.0
5	2.50	11.5499	3.1	.8	6.2100	2.9	.9	5.3399	3.9	2.0
6	2.95	11.2990	3.1	.8	6.1537	2.9	.9	5.1453	3.9	2.1
7	3.45	11.0996	3.1	.8	6.0201	2.9	.9	5.0715	3.9	2.0
8	4.10	10.8966	3.1	.8	5.9166	2.9	.9	4.9800	3.9	2.0
9	4.75	10.6526	3.1	.8	5.8183	2.9	.9	4.8344	3.9	2.1
10	5.50	10.4077	3.1	.8	5.7168	2.9	.9	4.6908	3.9	2.1
11	6.45	10.2010	3.1	.8	5.6113	2.9	.9	4.5897	3.9	2.1
12	7.45	9.9492	3.1	.8	5.5308	2.9	.9	4.4183	3.9	2.1
13	8.70	9.7217	3.1	.8	5.4356	2.9	.9	4.2861	3.9	2.2
14	10.10	9.4971	3.1	.8	5.3143	2.9	.9	4.1827	3.9	2.2
15	11.75	9.2713	3.1	.8	5.2141	2.9	.9	4.0572	3.9	2.2
16	13.60	9.0339	3.1	.8	5.0905	2.9	.9	3.9434	3.9	2.2
17	15.75	8.8101	3.1	.8	4.9576	2.9	.9	3.8525	4.0	2.2
18	18.25	8.5781	3.1	.8	4.8591	2.9	.9	3.7190	4.0	2.2
19	21.15	8.3306	3.1	.8	4.7509	2.9	.9	3.5797	4.0	2.3
20	24.50	8.1100	3.1	.8	4.6432	2.9	.9	3.4668	4.0	2.3
21	28.40	7.9116	3.1	.8	4.5184	2.9	.9	3.3932	4.0	2.3
22	32.90	7.6860	3.1	.8	4.3957	2.9	.9	3.2903	4.0	2.3
23	38.10	7.4688	3.1	.8	4.2984	2.9	.9	3.1704	4.0	2.3
24	44.10	7.2587	3.1	.8	4.1758	2.9	.9	3.0819	4.0	2.3
25	51.20	6.7805	3.1	.8	3.9180	2.9	1.0	2.8705	4.0	2.4
26	70.55	6.5780	3.1	.8	3.8007	2.9	1.0	2.7774	4.0	2.4
27	81.40	6.3777	3.1	.8	3.6897	2.9	1.0	2.6880	4.0	2.4
28	93.90	6.1868	3.1	.8	3.5790	2.9	1.0	2.6078	4.1	2.4
29	108.45	5.9907	3.1	.8	3.4616	2.9	1.0	2.5290	4.1	2.4
30	125.30	5.8160	3.1	.8	3.3509	2.9	1.0	2.4651	4.1	2.4
31	144.75	5.6116	3.1	.8	3.2465	2.9	1.0	2.3651	4.1	2.5
32	167.30	5.4318	3.1	.9	3.1454	2.9	1.1	2.2864	4.1	2.5
33	193.45	5.2593	3.1	.9	3.0398	2.9	1.1	2.2195	4.1	2.5
34	223.70	5.0988	3.1	.9	2.9480	2.9	1.1	2.1508	4.1	2.5
35	258.75	4.9355	3.1	.9	2.8569	2.9	1.1	2.0785	4.1	2.5
36	299.65	4.7709	3.1	.9	2.7608	2.9	1.1	2.0101	4.1	2.6
37	347.10	4.6103	3.1	.9	2.6715	2.9	1.1	1.9388	4.1	2.6
38	402.10	4.4701	3.1	.9	2.5852	2.9	1.1	1.8839	4.1	2.6
39	541.05	4.1564	3.1	.9	2.4115	2.9	1.2	1.7449	4.2	2.7
40	619.55	4.0170	3.1	.9	2.3331	2.9	1.2	1.6839	4.2	2.7
41	698.05	3.8911	3.2	.9	2.2678	2.9	1.2	1.6232	4.2	2.8
42	776.55	3.7899	3.2	.9	2.2011	2.9	1.2	1.5888	4.2	2.8
43	855.00	3.6947	3.2	.9	2.1411	2.9	1.2	1.5536	4.3	2.8
44	933.45	3.6125	3.2	.9	2.0958	2.9	1.2	1.5168	4.3	2.8
45	1011.90	3.5387	3.2	.9	2.0499	2.9	1.2	1.4888	4.3	2.8
46	1090.30	3.4520	3.2	.9	2.0116	2.9	1.3	1.4403	4.3	2.9
47	1248.90	3.3180	3.2	1.0	1.9291	2.9	1.3	1.3889	4.3	2.9
48	1792.10	3.0248	3.1	2.5	1.6771	2.9	2.2	1.3477	3.8	6.3
49	1997.10	2.9599	3.1	1.8	1.6619	2.9	2.6	1.2979	3.8	5.3
50	2788.30	2.5449	3.1	2.1	1.4561	2.9	1.6	1.0888	3.9	5.3
51	2995.05	2.4371	3.1	1.5	1.4296	2.9	1.7	1.0076	3.9	4.3
52	3636.70	2.2788	3.1	2.5	1.3423	2.9	1.6	.9366	3.9	6.4
53	4109.50	2.2375	3.1	2.1	1.2728	2.9	1.3	.9646	3.9	5.2
54	4318.10	2.1060	3.1	6.9	1.2427	2.9	1.4	.8633	4.0	16.9
55	4767.95	2.0733	3.1	1.3	1.2065	2.9	1.2	.8668	4.0	3.4
56	4967.60	2.1051	3.1	2.1	1.1761	2.9	1.2	.9290	4.0	5.1
57	5577.95	1.9743	3.1	1.9	1.1231	2.9	2.1	.8512	4.0	5.3
58	6207.05	1.8837	3.1	3.3	1.0833	2.9	1.6	.8004	4.0	5.8
59	7461.65	1.7894	3.2	2.6	.9850	2.9	2.4	.8034	4.1	6.5
60	8092.55	1.7099	3.2	1.6	.9475	2.9	1.9	.7625	4.1	4.2
61	8692.65	1.6703	3.2	2.0	.9240	2.9	1.4	.7462	4.2	4.7
62	9571.00	1.6257	3.2	2.0	.8838	2.9	3.5	.7419	4.2	6.0
63	10554.55	1.5471	3.2	1.6	.8576	2.9	1.0	.6896	4.2	3.9
64	13944.60	1.3736	3.2	1.5	.7357	2.9	2.7	.6379	4.3	4.4
65	16168.95	1.3004	3.2	1.2	.7027	2.9	2.6	.5977	4.3	4.0
66	18691.05	1.2392	3.3	2.0	.6605	2.9	2.4	.5787	4.3	5.2
67	21150.65	1.1776	3.3	1.9	.6309	2.9	1.3	.5467	4.4	4.3
68	23641.65	1.1235	3.3	1.2	.6040	2.9	1.4	.5195	4.4	3.1
69	26146.40	1.0733	3.3	1.7	.5785	2.9	1.4	.5027	4.4	3.9
70	31131.75	1.0001	3.3	1.4	.5450	2.9	2.7	.4552	4.5	4.4
71	36155.55	.9400	3.3	1.3	.5112	2.9	1.5	.4288	4.6	3.4
72	41119.55	.8838	3.3	1.3	.4865	2.9	1.4	.3973	4.6	3.4
73	46154.45	.8389	3.3	1.2	.4724	2.9	1.1	.3666	4.7	3.1
74	51122.30	.8001	3.3	1.7	.4613	2.9	3.1	.3389	4.8	5.8
75	61121.40	.7412	3.3	1.3	.4296	2.9	2.0	.3116	4.9	4.1
76	71149.86	.6979	3.4	1.2	.4018	2.9	1.2	.2961	5.1	3.3
77	91126.81	.6150	3.3	4.5	.3886	2.9	3.2	.2264	5.4	13.5
78	101147.72	.5976	3.4	2.0	.3567	2.9	.9	.2489	5.5	5.0
79	126148.61	.5316	3.4	2.0	.3243	2.9	1.2	.2073	5.5	5.4
80	151138.22	.4981	3.4	2.1	.3073	2.9	1.4	.1909	5.5	5.8
81	170530.16	.4744	3.4	1.1	.2922	2.9	1.8	.1821	5.5	4.1
82	181650.91	.4636	3.4	1.0	.2859	2.9	1.6	.1777	5.5	3.6
83	202656.56	.4409	3.3	1.1	.2795	2.9	2.1	.1614	5.5	4.8

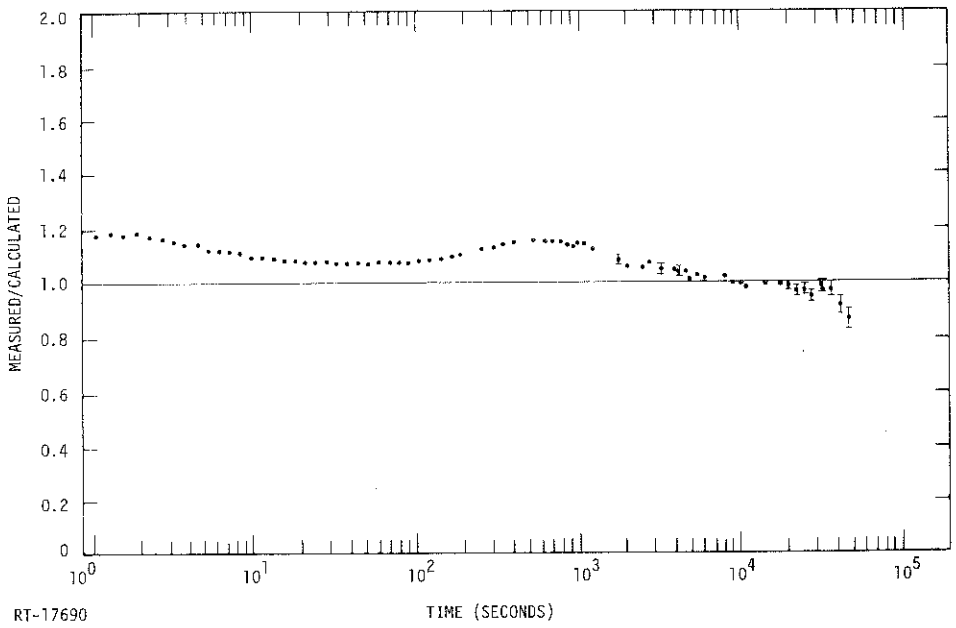

Figure 5-1. Ratio of measured to calculated total decay heat for ^{239}Pu for a 1000 second irradiation

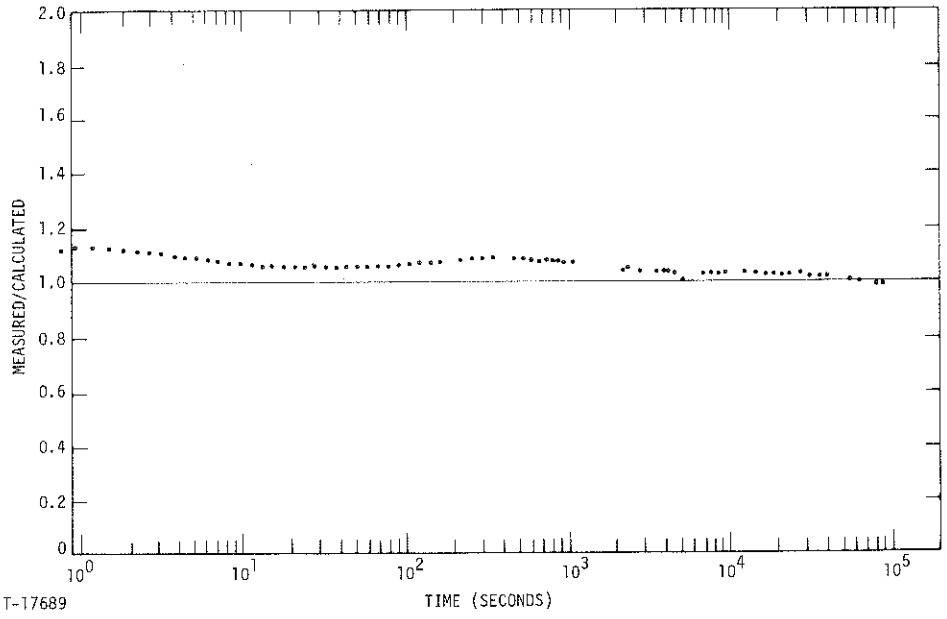

Figure 5-2. Ratio of measured to calculated total decay heat for ^{239}Pu for a 24-hour irradiation

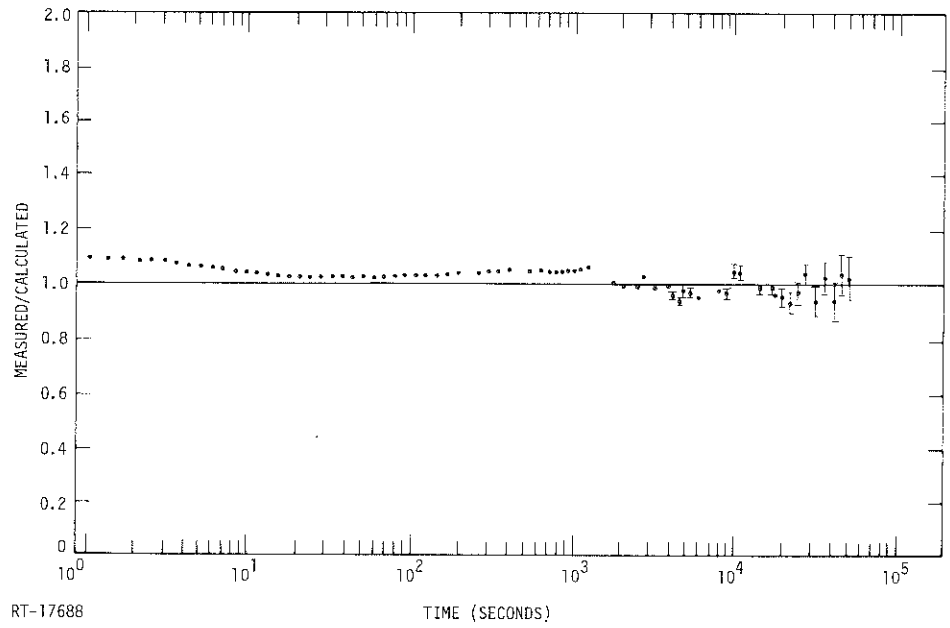

Figure 5-3. Ratio of measured to calculated total decay heat for ^{235}U for an irradiation of 1000 seconds

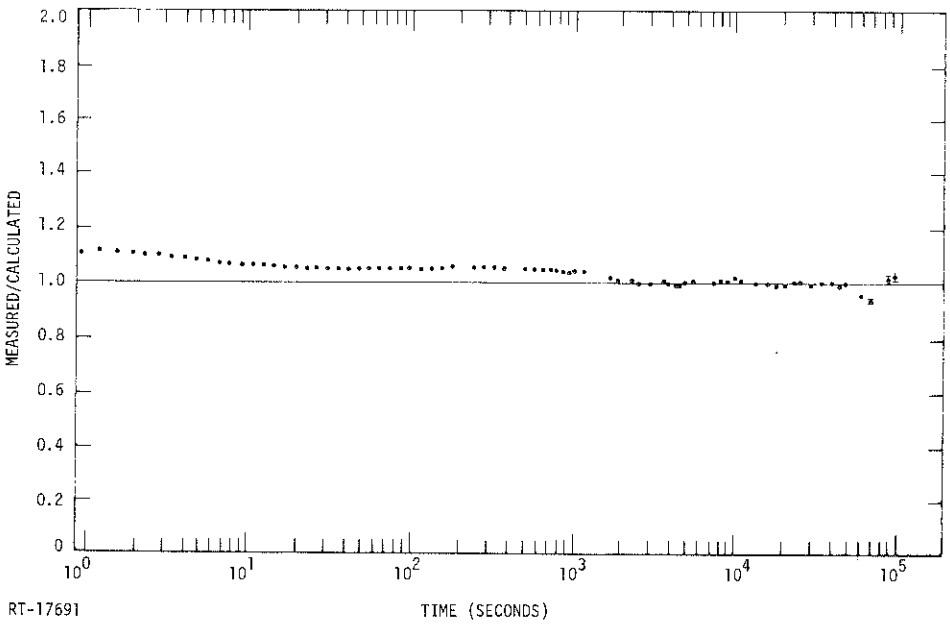

Figure 5-4. Ratio of measured to calculated total decay heat for ^{235}U for an irradiation of 20,000 seconds

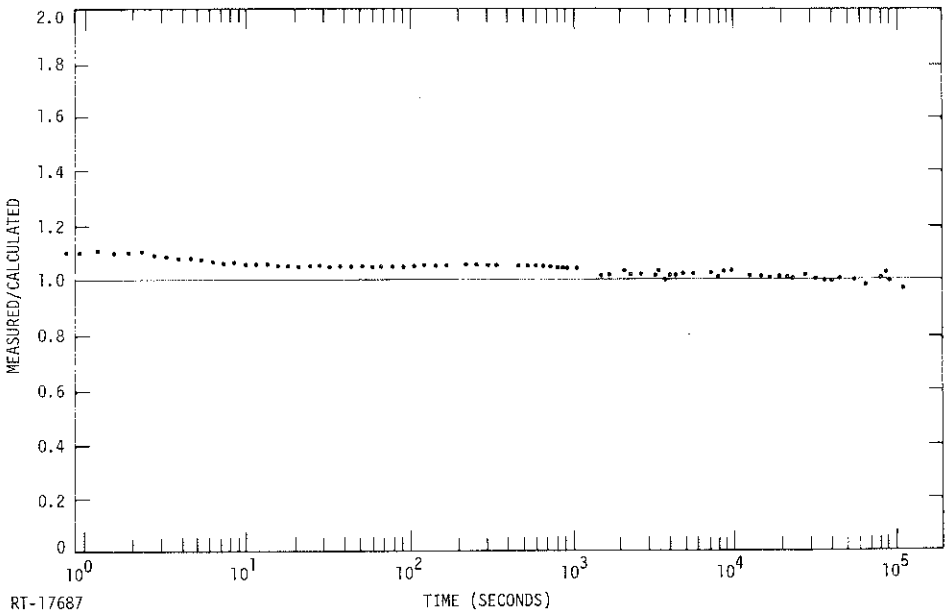

Figure 5-5. Ratio of measured to calculated total decay heat for ^{235}U for a 24-hour irradiation

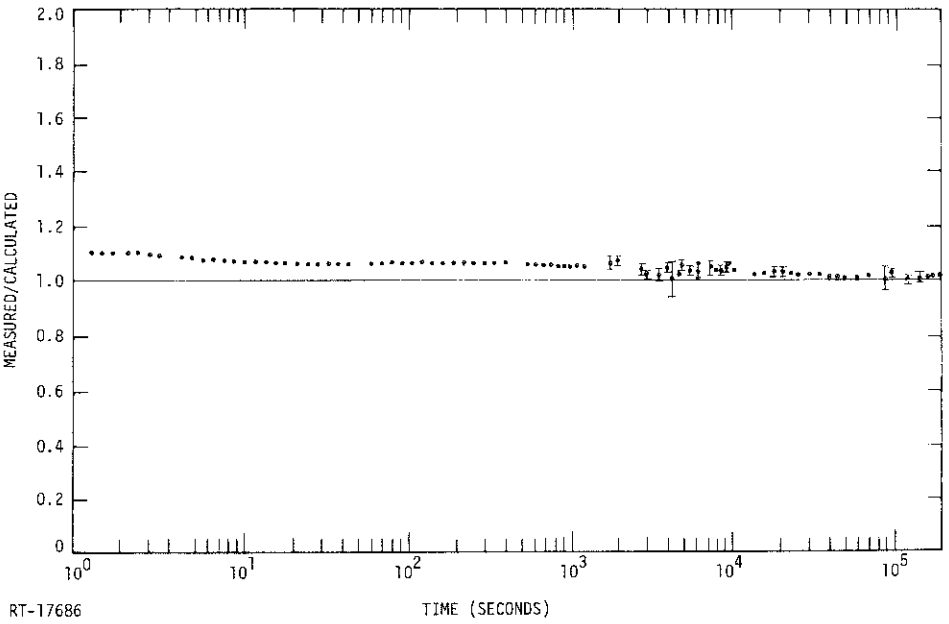

Figure 5-6. Ratio of measured to calculated total decay heat for ^{235}U for a 35-day irradiation

longer times as the uncertainties in the data library decrease. The 1000-second irradiation data drops below the calculation at approximately 1.5 hours cooling, while the 24-hour data remain about 2% high in the longer cooling time region. Figure 5-7 shows the separate beta and gamma-ray ratios with summation calculations for ^{239}Pu irradiated for 24 hours.

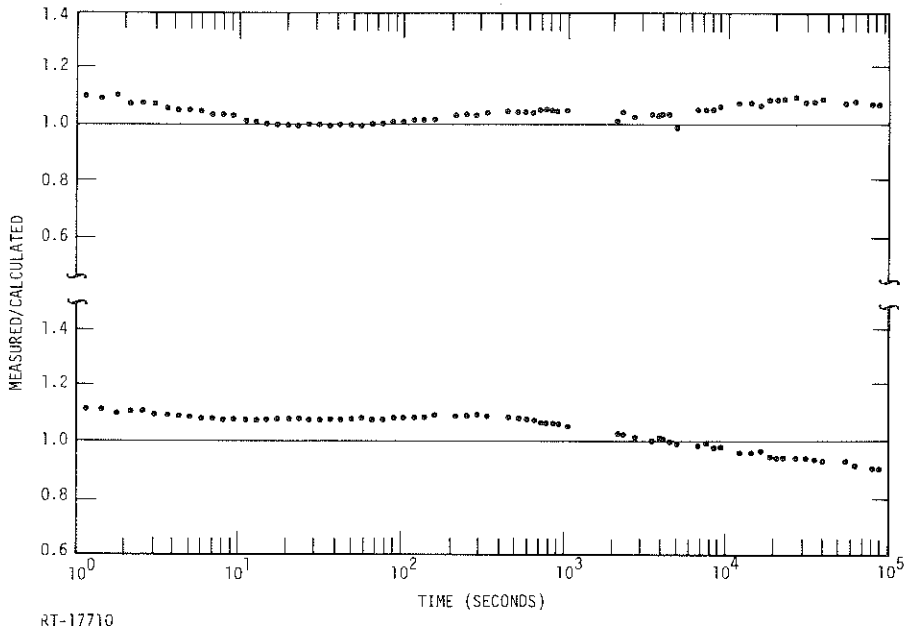

Figure 5-7. Ratio of measured to calculated decay power for separate beta (top) and gamma-ray (bottom) components of ^{239}Pu irradiated for 24 hours

The most significant discrepancy between measurement and calculation for ^{239}Pu occurs in the region 200-1000 s; at ~500 s the calculations are low by about 13% for the 1000 s irradiation. In the 24-h data this same region is also discrepant, but by a smaller margin (~8%). The two other recent measurements of ^{239}Pu decay heat (12, 26) also show this anomalous bump in the ratio of measurement to calculation around 500 s cooling (27). It is particularly interesting that this anomaly persists for three independent measurements, each at different irradiation times. The cause of this anomaly is undoubtedly incorrect or deficient data in the fission product library. The most obvious candidates for possible errors are the ^{239}Pu yields. However, recent examinations of ENDF/B-IV yield data and calculations with

the new version V yields indicate that the discrepancies are not due to the yields (27).

Looking at the individual components, it appears that the anomaly that occurs around 500 seconds is primary for the gamma component. Another result that appears in this figure is the apparent incorrect partitioning of the beta and gamma components at long times ($>10^4$ seconds). It is not possible to conclude whether the partitioning error is in the measurements or the calculations or both. It is known, however, that the summation calculations do not properly treat conversion electrons. The ENDF/B-IV fission product library lumps the conversion electron and x-ray energies in with the gamma-ray energy. This results in an incorrect partitioning of the decay energy between gamma rays and electrons in the summation calculations. For those radionuclides where significant decays are by internal conversion the effect of this approximation could be significant. At long cooling times the decay power is produced by relatively few nuclides. Thus it is possible that part of the partitioning error is due to the incorrect handling of the conversion electrons.

The 24-h irradiation ^{235}U data reported here represent improvements in the previously reported data for ^{235}U (7). Slight improvements have been made in the accuracy of the normalization, and significant improvements have been made in the energy loss corrections. The latter are the result of using more accurate beta and gamma spectral data corresponding to the irradiation conditions of the measurements.

A program to measure both beta and gamma spectra as a function of cooling time is currently underway at IRT. It is hoped that the source of at least some of the discrepancies noted in this work will be resolved. It is possible that the current measurements of fission product beta and gamma-ray spectra in the discrepant regions will shed some light on the discrepancies noted here.

In general, the data presented here are consistent with the other high quality results obtained for ^{235}U. For ^{239}Pu the situation is not as satisfactory. The discrepancy between calculation and experiment is undesirably large at short cooling times. The shapes of the cooling curves seem to be qualitatively similar to other recent measurements, but the present data disagree significantly in normalization with that reported in Reference 26.

Section 6

REFERENCES

1. M. A. Bjerke, J. S. Holm, M. R. Shay and B. I. Spinrad, "A Review of Short-Term Fission Product Decay Power," Nuclear Safety 18, 596-616 (1977).

2. V. E. Schrock, "A Revised ANS Standard for Decay Heat from Fission Products," International Meeting Nuclear Power Reactor Safety, Brussels, October 16-19, 1978.

3. F. Schmittroth, "Uncertainty Analysis of Fission-Product Decay-Heat Summation Methods," Nucl. Sci. Eng. 59, 117-139 (1976).

4. B. I. Spinrad, "The Sensitivity of Decay Power to Uncertainties in Fission Product Yields," Nucl. Sci. Eng. 62, 35-44 (1977).

5. F. Schmittroth and R. E. Schenter, "Uncertainties in Fission-Product Decay-Heat Calculations," Nucl. Sci. Eng. 63, 276-291 (1977).

6. F. M. Nuh and S. G. Prussin, "Uncertainties in Decay Power from Summation Calculations," Proc. Topical Meeting on Thermal Reactor Safety, Sun Valley, Idaho, August 1977, CONF 770708, Vol. 2, pp. 227-239.

7. S. J. Friesenhahn, N. A. Lurie, V. C. Rogers and N. Vagelatos, "^{235}U Fission Product Decay Heat from 1 to 10^5 Seconds," EPRI NP-180, prepared by IRT Corporation for the Electric Power Research Institute (February 1976).

8. J. K. Dickens and J. W. McConnell, "Determination of the Number of Fissions Created in a Sample of ^{239}Pu during a 24-hour Irradiation at the IRT Corporation ^{252}Cf Facility," EPRI NP-997, Oak Ridge National Laboratory (February 1979).

9. E. Haddad, R. B. Walton, S. J. Friesenhahn and W. M. Lopez, "A High Efficiency Detector for Neutron Capture Cross Section Measurements," Nucl. Instr. and Meth. 31, 125-138 (1964).

10. S. J. Friesenhahn, "Light Collection from Large Cylindrical Scintillators," Rev. Sci. Instr. 42, 1016-1030 (1971).

11. S. J. Friesenhahn and N. A. Lurie, "Measurements of Fission Product Decay Heat for ^{235}U and ^{239}Pu," Proc. Topical Meeting on Thermal Reactor Safety, Sun Valley, Idaho, August 1977, CONF 770708, Vol. 2, pp. 163-177.

12. J. K. Dickens, J. F. Emery, T. A. Love, J. W. McConnell, K. J. Northcutt, R. W. Peelle, and H. Weaver, "Fission Product Energy Release for Times Following Thermal-Neutron Fission of ^{239}Pu Between 2 and 14000 Seconds," ORNL-NUREG-34, Oak Ridge National Laboratory (April 1978).

13. V. E. Schrock, L. M. Grossman, S. G. Prussin, K. C. Sockalingam, F. M. Nuh, C. K. Fan, N. Z. Cho, and S. J. Oh, "A Calorimeter Measurement of Decay Heat from ^{235}U Fission Products from 10 to 10^5 Seconds," EPRI NP-616, prepared by University of California Berkeley for Electric Power Research Institute (February 1978).

14. B. I. Spinrad, Private communication, 1977.

15. H. M. Colbert, "SANDYL: A Computer Program for Calculating Combined Photon-Electron Transport in Complex Systems," SLL-74-0012, Sandia Laboratories (1974).

16. T. R. England and M. S. Stamatelatos, "Beta and Gamma Spectra and Total Decay Energies from Fission Products," Trans. Am. Nucl. Soc. 23, 493 (1976).

17. M. S. Stamatelatos and T. R. England, "FPDCYS and FPSPEC: Computer Programs for Calculating Fission-Product Beta and Gamma Multigroup Spectra from ENDF/B-IV Data," LA-NUREG-6818-MS, Los Alamos Scientific Laboratory (May 1977).

18. Fission-Product Decay Library of the Evaluated Nuclear Data File, Version IV (ENDF/B-IV). Available from, and maintained by the National Nuclear Data Center at Brookhaven National Laboratory.

19. T. R. England and R. S. Schenter, "ENDF/B-IV Fission Product Data Files: Summary of Major Nuclide Data," LA-6116-MS(ENDF-223), Los Alamos Scientific Laboratory (1975).

20. T. R. England and M. S. Stamatelatos, "Multigroup Beta and Gamma Spectra of Individual ENDF/B-IV Fission Product Nuclides, "LA-NUREG-6622-MS, Los Alamos Scientific Laboratory (December 1976).

21. T. R. England and M. S. Stamatelatos, "Comparisons of Calculated and Experimental Delayed Fission-Product Beta and Gamma Spectra from ^{235}U Thermal Fission," LA-NUREG-6896-MS, Los Alamos Scientific Laboratory (July 1977).

22. T. R. England, Private communication (correspondence T. R. England to N. A. Lurie and S. J. Friesenhahn, April 21, 1976; October 18, 1976; November 29, 1976, and November 8, 1977).

23. T. J. Trapp, S. M. Baker, A. W. Prichard and B. I. Spinrad, "ROPEY: A Computer Code to Evaluate the Fission Product Shutdown Decay Heat and Its Uncertainties," OSU-NE-7701, Oregon State University (August 1977).

24. T. R. England, "CINDER - A One Point Depletion and Fission Product Program," WAPD-TM-334 (Rev.), Bettis Atomic Power Laboratory (1964); T. R. England, R. Wilczynski and N. L. Whittemore, "CINDER-7: An Interim Report for Users," LA-5885-MS, Los Alamos Scientific Laboratory (April 1975).

25. J. K. Dickens, J. F. Emery, T. A. Love, J. W. McConnell, K. J. Northcutt, R. W. Peelle and H. Weaver, "Fission-Product Energy Release for Times Following Thermal-Neutron Fission of ^{235}U Between 2 and 14,000 Seconds," ORNL-NUREG-14, Oak Ridge National Laboratory (1977).

26. J. L. Yarnell and P. J. Bendt, "Calorimetric Fission Product Decay Heat Measurements for ^{239}Pu, ^{233}U and ^{235}U," NUREG/CR-0349 (LA-7452-MS), Los Alamos Scientific Laboratory (September 1978).

27. T. R. England, R. E. Schenter and F. Schmittroth, "Integral Decay-Heat Measurements and Comparisons to ENDF/B-IV and V," NUREG/CR-0305 (LA-7422-MS), Los Alamos Scientific Laboratory (August 1978).

EPRI NP-998

September 1979

Decay Power From ^{239}Pu and ^{235}U Fission Products